SYSTEM-SCALE GEOMORPHOLOGY AND VEGETATION MONITORING REPORT

2017 - 2024

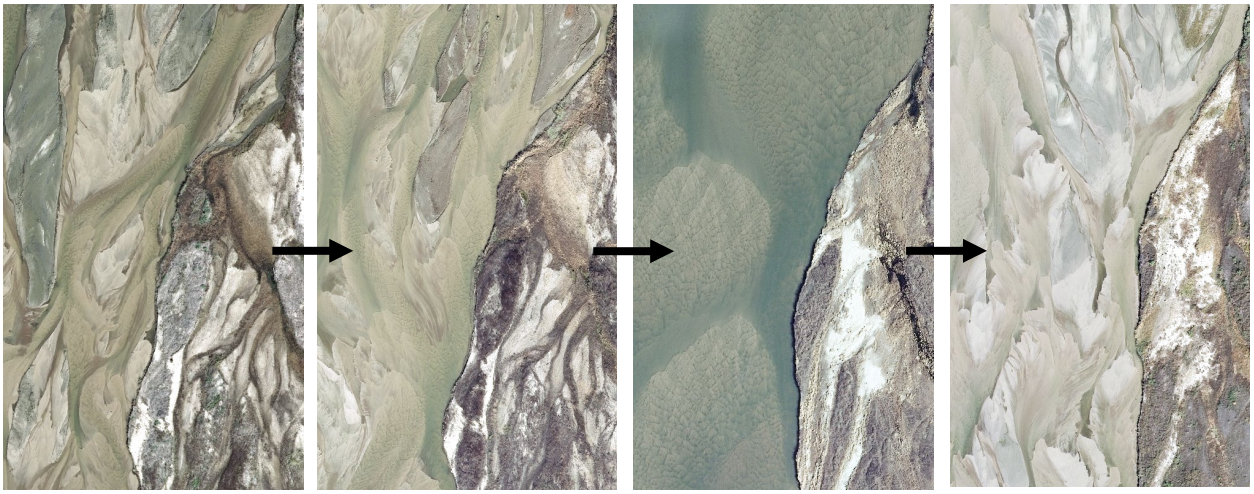

Prepared for: PRRIP Governance Committee
Date: 7/10/2025

Prepared By
Executive Director's Office
Platte River Recovery Implementation Program
4111 4th Avenue, Suite 6
Kearney, NE 68845

Suggested Citation:
Executive Director's Office. 2025. Platte River Recovery Implementation Program: 2024 System-Scale Geomorphology and Vegetation Monitoring Report 2017-2024.

Executive Summary

This report presents the results of the Platte River Recovery Implementation Program's (PRRIP) system-scale geomorphology and vegetation monitoring effort from 2017 to 2024. The goal of this monitoring is to assess long-term trends in river morphology, in-channel vegetation, and habitat conditions within the Associated Habitat Reach (AHR) of the central Platte River—an area critical to the PRRIP's target species, especially the whooping crane.

To achieve this goal, the Program implemented an integrated remote sensing-based monitoring approach beginning in 2017, utilizing high-resolution aerial imagery and topo-bathymetric LiDAR to produce annual datasets. These data were used to generate detailed land cover classifications, hydrodynamic model outputs, sediment volume change estimates, and a range of habitat metrics, including maximum and total unobstructed channel width and wetted width at biologically relevant flows.

The report documents change in key physical and ecological drivers such as flow magnitude and timing, mechanical vegetation management, sediment augmentation, and flow consolidation. It also presents metrics that reflect the effectiveness of these interventions in maintaining or improving habitat conditions. System-wide trends are reported for both managed and unmanaged channel segments, allowing a preliminary evaluation of management effectiveness.

The data and analyses in this report support adaptive management under the Extension Science Plan by informing progress toward PRRIP's management objectives and providing data used to address Extension Big Questions—particularly those related to whooping crane habitat suitability and the effects of sediment and flow management actions.

Table of Contents

List of Figures

List of Tables

List of Acronyms

2D	Two dimensional
AHR	Associated Habitat Reach
AMP	Adaptive Management Plan
Cfs	Cubic feet per Second
CY	Cubic Yards
DoDs	Digital Elevation Model of Difference
EDO	Executive Directors Office
GIS	Geographic Information System
GPS	Global Positioning System
ISAC	Independent Scientific Advisory Committee
J2 Return	Johnson No. 2 Hydropower Return
LiDAR	Light Detection and Ranging
MUCW	Maximum unobstructed channel width
NDVI	Normalized Difference Vegetation Index
NDWI	Normalized Difference Water Index
PRRIP	Platte River Recovery Implementation Program
QSI	Quantum Spatial Inc
TUCW	Total Unobstructed Channel Widths
USGS	United States Geological Survey

Introduction

The Platte River Recovery Implementation Program (PRRIP or Program) is responsible for implementing aspects of the recovery plan for four threatened and endangered species. Three of those species occur in the central Platte including the now recovered (federally delisted) interior least tern (*Sterna antillarum athalassos*), threatened piping plover (*Charadrius melodus*), and highly endangered whooping crane (*Grus americana*). In the central Platte, piping plovers and interior least terns forage along the channel and infrequently nest on mid-channel sandbars, primarily those constructed to provide nesting habitat. In 2016, the Program shifted management focus for these species to off-channel sand and water habitat.[1] As such, Extension Science Plan[2] (PRRIP 2022a) priorities relate to habitat suitability and productivity at off-channel sand and water habitat sites.

In contrast, the Program concentrates on establishing and preserving highly suitable riverine habitat for whooping cranes. Performance indicators include increasing the area of suitable whooping crane roosting and foraging habitat. Research and monitoring conducted during the First Increment (2007-2019) and First Increment Extension (using additional data through spring of 2022) suggest width of channel unobstructed by dense vegetation and the distance to nearest forest are the best indicators of roosting habitat suitability (PRRIP 2017; Baasch et al., 2019; PRRIP 2025). The system-scale geomorphology and vegetation monitoring report documents trends in channel morphology, vegetation, and whooping crane habitat suitability metrics in relation to natural hydrology, flow releases, and in-channel mechanical management actions. This information is used by the Program to assess our ability to create and maintain highly suitable whooping crane habitat under a broad range of environmental conditions.

From 2009 – 2016 the Program implemented a field-based monitoring protocol that included topographic transect surveys, vegetation plot surveys, and sediment size/transport sampling (Tetra Tech 2017). That approach was changed to a remote sensing approach after 2016 due to concerns about low spatial coverage, increasing cost and the recognition that much of the vegetation and sediment data was not useful for addressing priority uncertainties (ISAC 2014). In 2017, the Program pivoted to a remote-sensing approach based around collection and analysis of high-resolution aerial imagery and topo-bathymetric Light Detection and Ranging (LiDAR) data. To our knowledge, this is the first-time collection and analysis of high resolution aerial topo-bathymetric LiDAR has been conducted at this scale and frequency. Consequently, data collection and analysis methods had to be developed from the ground-up. The Executive Director's Office (EDO) spent much of 2017-2020 collaborating with the Program's remote sensing contractor, NV5 (formerly Quantum Spatial) and working internally to develop and refine analysis methods that could be applied annually at a system scale.

The current remote-sensing data collection and analysis protocol is attached as **Appendix A**. Protocol implementation includes object-based classification of in-channel land cover to

[1] The Program also maintains ten (10) acres of on-channel Moving Complex Approach (MCA) nesting habitat in the Associated Habitat Reach.

[2] The First Increment AMP has been updated and renamed Extension Science Plan.

characterize changes in in-channel vegetation. The results of this analysis are reported relative to Extension Science Plan learning priorities (PRRIP 2022a).

Scope of Analysis and Reporting Scales

The Platte River is a major tributary to the Missouri River with a contributing drainage area of approximately 71,000 square miles (**Figure 1**). The headwaters of the North and South Platte Rivers are in the Rocky Mountains and flow eastward to their confluence near North Platte, NE. The central Platte River extends downstream from that point to the Loup River confluence near Columbus, NE. The 90-mile stretch of the Big Bend reach of the central Platte River from Lexington, NE to Chapman, NE is the focus area for Program implementation and is referred to as the Associated Habitat Reach (AHR).

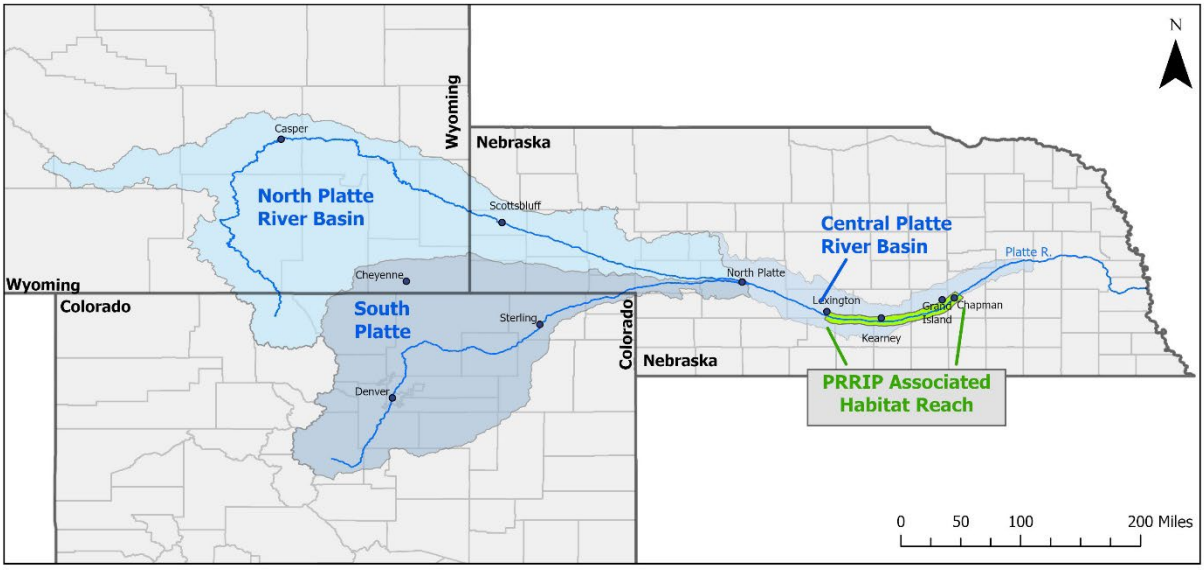

Figure 1. Map of the central and upper Platte River basin including the Program's Associated Habitat Reach (AHR) where management actions are implemented to benefit target species.

Analyses were conducted for the entire AHR and are generally reported at three spatial scales: the entire AHR, by geomorphic reach, and whether an area is being managed by the Program or other organizations to benefit target species. AHR-scale metrics are reported as averages to capture reach-wide annual trends. The reach upstream of Overton is split into north and south channel segments because the two channels are hydrologically and hydraulically disconnected from each other for most of the reach.

Geomorphic reaches are adapted from work by Fotherby (2009) that grouped segments with similar hydrology and channel morphology. The Fotherby segment designations were modified slightly by combining reaches 3D and 4A[3] (**Table 1** and **Figure 2**) to produce ten (10) geomorphic reaches. Several geomorphic reaches have major flow splits or areas of substantial anastomosing. In those

[3] These reaches were split in the original Fotherby (2009) analysis due to differences in historical floodplain width. They are combined here because the morphology of the contemporary channel is similar across the two reaches.

reaches, results are reported for all channels together and the main channel individually[4]. For this report, the main channel is identified as either the 1) channel with the majority of flow or 2) channel managed to provide whooping crane habitat in segments like Mormon Island where shifts in flow distribution through time have resulted in side channels carrying more flow than the main channel.

Management-scale analyses compare channel characteristics of segments of the main channel that are maintained or managed to benefit target species to those that are not (**Figure 2**). Managed areas include segments of channel managed by PRRIP and other groups including The Crane Trust, The Audubon Society (Rowe Sanctuary), The Nature Conservancy (TNC) (Urdil), Central Nebraska Public Power and Irrigation District (CNPPID) (Jeffrey Island), and the Nebraska Public Power District (NPPD) (Cottonwood Ranch).

Table 1. Geomorphic Reach designations of the AHR listed from west to east (upstream to downstream), adapted from Fotherby (2009).

Reach Code	Reach Name	Reach Length (mi)	Geomorphic Description of Channel	% Flow in Main Channel
Reach 1	North channel from Lexington to Overton	11.3	Wandering: Unconsolidated and heavily vegetated overbank.	N/A
Reach 2	South channel J2 Return to Overton	7.5	Meandering: Incised as much as 25 feet and void of incoming bedload.	N/A
Reach 3A	Overton to Elm Creek	8.7	Flow split by large islands. Main channel braided and anastomosed.	50%
Reach 3B	Elm Creek to Odessa	7	Braided and anastomosed.	100%
Reach 3C	Odessa to Kearney	8.9	Braided and anastomosed.	85%
Reach 3D/4A	Kearney to Gibbon	15.3	Flow split by large islands. Main channel braided.	53%
Reach 4B	Gibbon to Wood River	9.7	Braided and island braided.	81%
Reach 4C	Wood River to Alda	8.9	Flow split by large islands. Main channel mostly braided.	87%
Reach 4D	Alda to Grand Island	11.7	Flow split by large islands. Main channel mostly braided.	21%
Reach 5	Grand Island to Chapman	10.3	Alternating braided and anastomosed.	100%

[4] Suitable whooping crane habitat rarely occurs in side channels due to inadequate unobstructed width.

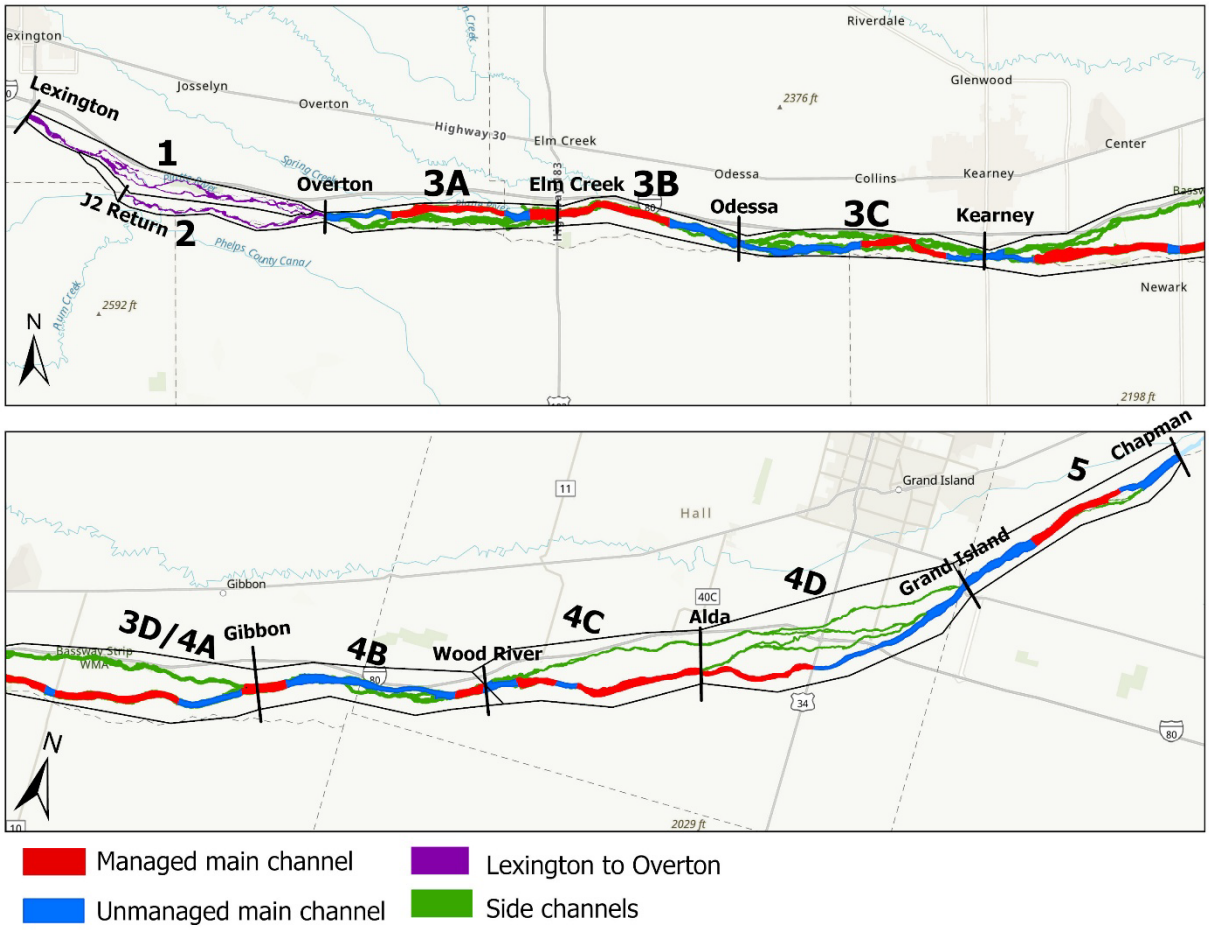

Figure 2. Map of the Associated Habitat Reach (AHR) includes geomorphic reaches (1-5), main and side channels, main channel areas that are managed to reduce in-channel vegetation, and other unmanaged main channel areas.

Merging Field and Remote Sensing Data and Analyses

The Program has collected and analyzed both field and remote sensing data since 2009. In many cases, field and remote-sensing based protocols involve quantification of similar or identical metrics. However, the underlying spatial coverage, data collection methods, and analyses are quite different. It is important that the Program can visualize and assess trends since the inception of monitoring. It is also important to identify and avoid situations where changes in methodology could lead to interpretive errors. As such, this report presents annual data for the entire system-scale monitoring period of 2009-2024 with the data separated by protocol where the metrics and results are comparable.

Mechanical Management

The Program and other organizations mechanically manage in-channel vegetation on both a site and system scale to maintain channel width and provide highly suitable whooping crane roosting habitat. System-scale management actions include helicopter application of herbicide to control

invasive vegetation (principally *Phragmites australis,* hereafter *Phragmites*) and sediment augmentation downstream of the J2 Return to halt channel incision and narrowing in the upper portion of the AHR. Site-scale management actions include clearing of trees from the AHR and disking of herbaceous vegetation on sandbars and along bank edges. These actions are taken to increase unvegetated channel width and promote channel widening through lateral erosion (Bankhead 2012).

It is important to track these actions to 1) assess their effectiveness, and 2) account for them in analyses of the relationship between natural drivers (such as hydrology) and channel response. Specific management metrics include the spatial extent of annual spraying, woody vegetation clearing and disking as well as the volume of sediment (cubic yards and tons) augmented each year.

Mechanical Management Analysis Methods

The Program maintains a Geographic Information System (GIS) geodatabase of the spatial extent of vegetation management actions and sediment augmentation implementation areas. **Table 2** provides the source of GIS data used to document annual management actions in that database. Aerial herbicide application is accomplished by helicopter with boom-mounted global positioning system (GPS) that records the spatial extent of application. Tree clearing and disking areas are recorded via GPS field surveys and track-logs and are then validated with orthorectified imagery collected twice each year. Rules for inclusion/exclusion from calculations are as follows:

- Tree clearing typically occurs adjacent to the active channel for the purpose of increasing whooping crane habitat suitability. All tree clearing was included whether it was inside the active channel or not.
- Disking occurs in and along the edge of the active channel for the purpose of increasing whooping crane habitat suitability. Disking polygons were clipped to the extent of the main channel (including banklines). Aerial herbicide application was clipped to the same extent.
- Sediment augmentation area and volumes for each year are calculated using pre- and post-augmentation LiDAR data collected by the Program. Augmentation quantities are validated using RTK-GPS, and area (acres) and volumes (cubic yards/tons) are calculated using a cut-fill routine in GIS software.

Table 2. Data source for documentation of annual system and site scale management actions.

Management Action	Data Source
Aerial Herbicide Application	Helicopter applicators equipped with boom-mounted GPS
Tree Clearing	GPS field surveys validated with Program Imagery
Disking	GPS track-logs validated with Program Imagery
Sediment Augmentation	Pre- and post-augmentation topo-bathy LiDAR surveys

Mechanical Management Results

Mechanical management during the period of 2007-2024 is presented in **Figure 3**. Since 2007, the area of disking and tree clearing each year has been a function of 1) proliferation of in-channel vegetation and 2) acquisition and restoration of new habitat lands. Application of aerial herbicide to control *Phragmites* began in 2007 and peaked in 2008, with almost 2,300 acres being sprayed.

Since 2009, annual spraying has been below 1,000 acres due to varying rates of *Phragmites* expansion and ability to implement large-scale spraying operations.

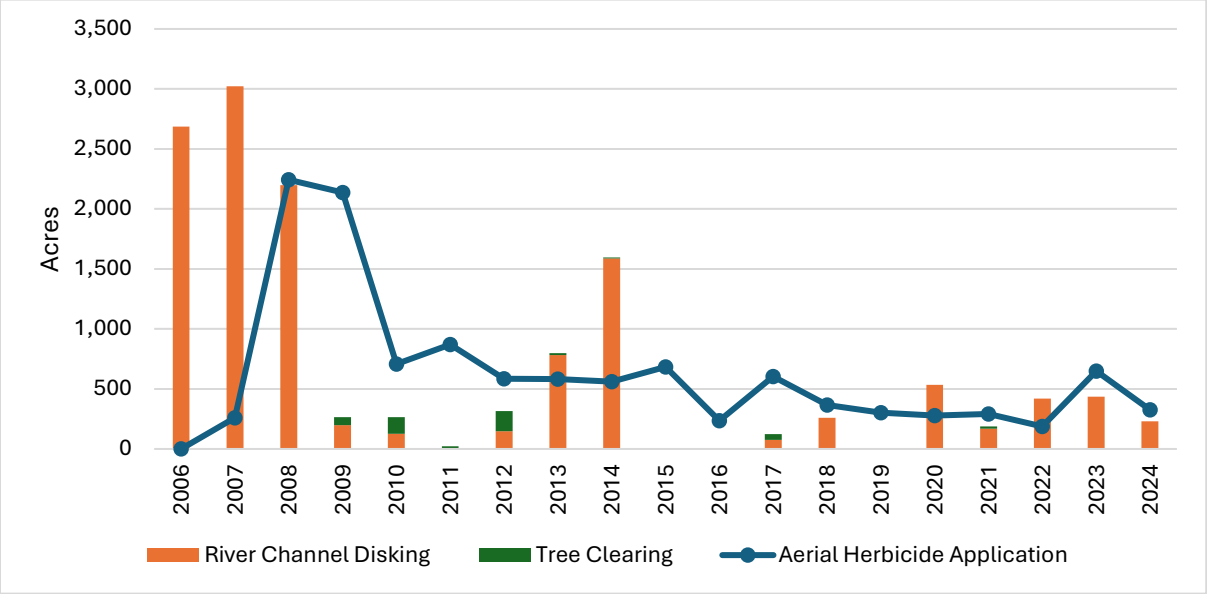

Figure 3. Total area of tree clearing, disking and spraying (aerial herbicide application) of the main channel by year for the AHR. Disking and spraying includes actions only in the active channel as well as along banklines.

The Program implemented a trial-scale sediment augmentation experiment in 2012-2013 that evaluated the effectiveness of pumping versus mechanical augmentation methods. Pumping was conducted at the Dyer Tract upstream of the Overton Bridge just downstream of the clearwater J2 return and mechanical augmentation was conducted further downstream after the confluence of the north channel and J2 return channel at Cottonwood Ranch in the Overton to Elm Creek bridge segment. A full-scale sediment augmentation experiment was conducted from 2017 -2022 with augmentation occurring at the upper end of the J-2 Return channel. **Table 3** provides the volume of sediment augmented by year (PRRIP, 2023).

Table 3. Sediment augmentation volume and location 2017 to 2024.

Year	Augmented (CY)	Augmented (tons)	Location
2012-2013	125,000	182,000	Dyer Tract and Cottonwood Ranch
2017	23,000	34,500	J-2 Return (South Channel)
2018	42,900	64,305	J-2 Return (South Channel)
2019	42,300	63,500	J-2 Return (South Channel)
2020	57,700	86,475	J-2 Return (South Channel)
2021	51,300	76,982	J-2 Return (South Channel)
2022	43,900	65,789	J-2 Return (South Channel)
2023	No Aug	No Aug	N/A
2024	No Aug	No Aug	N/A

Hydrologic Analysis

River flow (or discharge) is a primary driver of annual changes in channel characteristics on the Platte (Murphy et al., 2004, Farnsworth et al., 2018). The magnitude, timing, and duration of flows drive complex relationships between channel morphology, in-channel vegetation and sediment transport. For example, high peak flows in any season can laterally erode vegetated sandbars and banks. Lower flows sustained over a long period in the growing season can suppress the germination of seeds in the channel. Both influence unvegetated width of the channel, though through different physical processes. The hydrologic metrics included in this report have all been hypothesized to have distinct spatiotemporal effects on in-channel habitat.

Hydrologic Metrics

Priority hydrologic metrics are presented in **Table 4**. Priority metrics including mean annual discharge (Q_{AVG}), annual flow volume (V_{af}) and peak flow discharge/return interval (Q_P/Q_{Py}) are indicators of general hydrologic conditions in the reach. The Annual 40-day maximum flow ($Q_{Max\ 40}$) has been found to be a good predictor of increases in unvegetated channel width (PRRIP, 2017) and mean June flow (Q_{June}) is hypothesized to be a good predictor of channel width maintenance in years absent large peak flow events.

Table 4. Priority hydrologic metrics, symbols, and importance.

Metric	Metric Symbol	Utility
Mean Annual Discharge (cfs)	Q_{AVG}	Indicator of general hydrologic conditions
Annual Flow Volume (AFY)	V_{af}	Indicator of general hydrologic conditions
Annual Mean Daily Peak Discharge (cfs)	Q_P	This is the annual peak flow discharge. Mean daily flow is used because it occurs for a sufficient duration to do work within the channel.
Annual Peak Flow Return Interval (years)	Q_{Py}	Indicator of how frequently peak flow magnitudes occur
Annual 40-Day Maximum Flow (cfs)	$Q_{Max\ 40}$	Indicator of peak flow magnitude-duration relationship; good predictor of unvegetated channel width increases
Mean June Flow (cfs)	Q_{June}	Hypothesized to be good predictor of unvegetated channel width maintenance in absence of peak flow events

Hydrologic Analysis Methods

Mean daily discharge records were downloaded for three United States Geological Survey (USGS) stream gages located at Overton (06768000), Kearney (06770200), and Grand Island (06770500) for the period of 1958-2024.[5] Annual metric values were calculated for each gage location as follows:

- Mean annual discharge (cfs): Mean of average daily discharges for calendar year.
- Annual flow volume (acre-ft): Total volume of water passing gage in calendar year.

[5] Analysis started in 1958 as it marked the completion of the last major dam (Glendo) in the basin.

- Annual mean daily peak discharge (cfs): Maximum mean daily flow recorded at gage during calendar year.
- Annual peak flow return interval (years): Average time between occurrences of a specific instantaneous peak discharge as calculated using the methodology from USGS Bulletin #17B (Interagency Advisory Committee on Water Data, 1982). Method involves fitting historical data to a Log-Peason Type III distribution adjusted for 1) outlier values and 2) regional skewedness.
- Annual 40-Day maximum flow (cfs): Maximum of 40-day running mean discharge during calendar year.
- Mean June flow (cfs): Average of mean daily discharge values during the month of June.

Hydrologic Analysis Results

Mean daily discharge at the Grand Island gage (06770500) for the period of geomorphology and vegetation monitoring (2009-2024) is plotted in **Figure 4** as an example of the range of discharges observed since initiation of monitoring.[6] **Tables 5, 6** and **7** provide summaries of flow metrics for each of the USGS stream gages in the reach. During this period, the mean daily discharge across all gages ranged from a low of 570 cfs at Kearney in 2022 to a high of 4,214 cfs at Grand Island in 2011. Mean daily peak discharge ranged from a low of 2,290 cfs at Kearney in 2022 to a high of 19,600 cfs at Kearney in 2019. The 2019 Kearney peak had a return interval of 27.5 years. Other notable peaks included a long-duration peak in 2011 with an approximately 5-year return interval at all gages. In 2013 at Overton the peak return interval was 10.5 years and 4.8 years at Grand Island and 2015 peaks with over 15-year return intervals at all gages – 18 years at Overton, 15.1 years at Kearney, and 16.3 years at Grand Island. All large peaks occurred in late spring except for the 2013 event which occurred in the fall due to a historic precipitation event in the upper South Platte basin. The median of the mean daily peak discharge across all gages for the reporting period is 7,275 cfs at Grand Island.

[6] Grand Island plotted as it is the gage where target flow deficits/excesses are quantified and Program water projects are scored.

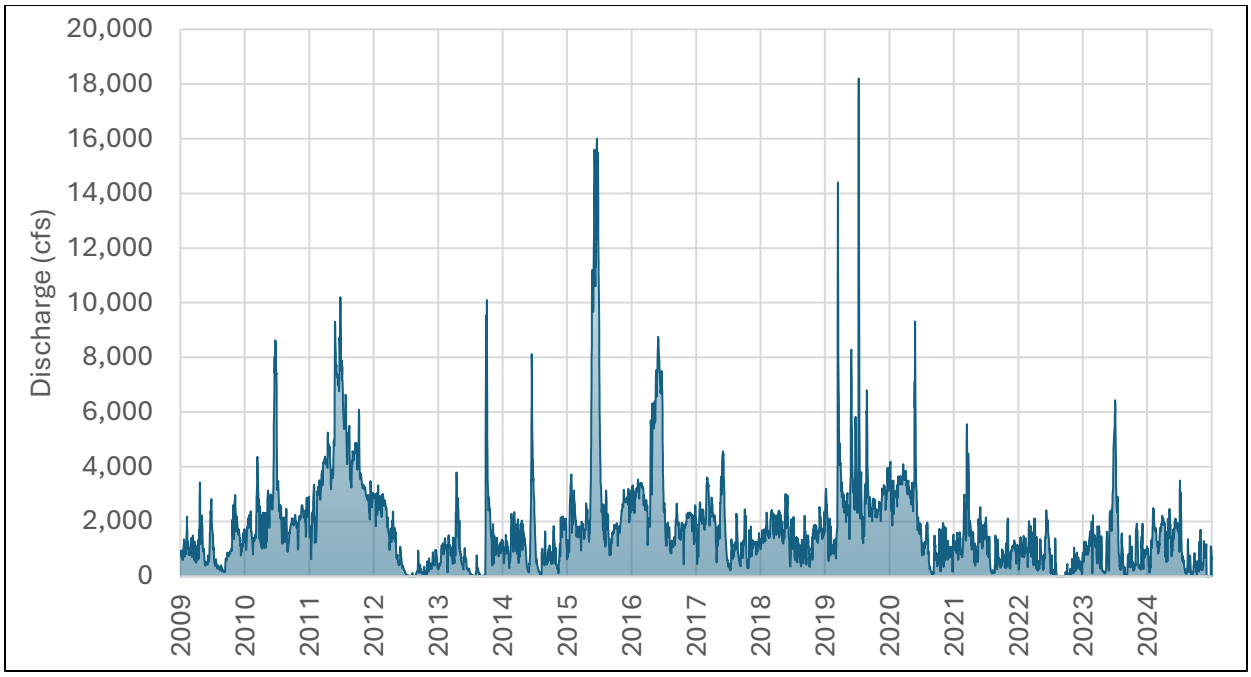

Figure 4. Mean daily discharge at the USGS Grand Island gage (06770500) for the period of 2009 through 2024.

Table 5. Summary of flow metrics at the USGS Overton (06768000) gage including mean annual value for period of 1958-2024 and annual values from 2009 to 2024.

Water Year	Mean Annual Discharge	Annual Volume (ac-ft)	Mean Daily Peak Discharge	Return Interval (Years)	40-Day Max Discharge	Mean June flow (germination)
1958-2024	1,660	1,202,733	6,224	2.8	3,757	2,670
2009	942	681,929	3,600	1.5	1,811	1,282
2010	2,157	1,561,636	7,370	3.6	4,108	4,536
2011	3,877	2,807,022	8,720	4.9	7,503	7,675
2012	1,114	808,918	3,430	1.4	2,796	319
2013	1,140	824,993	12,400	10.5	4,129	303
2014	1,249	904,100	7,360	3.6	3,150	3,822
2015	3,506	2,538,111	15,300	18.0	12,708	12,920
2016	2,950	2,141,887	8,600	4.8	7,364	6,433
2017	1,550	1,122,462	4,440	1.8	2,768	2,069
2018	1,415	1,024,114	2,960	1.3	1,834	1,343
2019	2,274	1,646,138	9,750	6.0	3,089	2,822
2020	1,800	1,306,550	3,820	1.6	2,977	1,966
2021	1,011	731,760	2,540	1.2	1,676	1,676
2022	646	467,461	2,300	1.2	1,383	1,533
2023	1,139	824,452	6,570	3.0	3,702	3,348
2024	975	708,151	2,370	1.2	1,591	1,553

Table 6. Summary of flow metrics at the USGS Kearney (06770200) gage including mean annual value for period of 1958-2024 and annual values from 2009 to 2024.

Water Year	Mean Annual Discharge	Annual Volume (ac-ft)	Mean Daily Peak Discharge	Return Interval (Years)	40-Day Max Discharge	Mean June flow (germination)
1958-2024	1,715	1,241,345	6,662	2.8	3,863	2,907
2009	916	663,347	3,270	1.4	1,761	1,761
2010	2,069	1,498,046	8,430	4.0	4,710	4,710
2011	3,972	2,875,716	9,100	4.6	7,694	7,694
2012	1,032	749,194	3,250	1.4	2,906	2,906
2013	1,068	773,442	12,000	7.8	3,803	3,803
2014	1,177	852,161	6,900	2.9	2,961	2,961
2015	3,304	2,392,003	15,900	15.1	12,413	12,413
2016	2,904	2,107,851	8,710	4.2	7,299	7,299
2017	1,499	1,085,145	4,380	1.7	2,697	2,697
2018	1,408	1,019,298	2,520	1.2	1,965	1,965
2019	2,550	1,845,975	19,600	27.5	3,976	3,976
2020	1,823	1,323,115	4,400	1.7	3,204	3,204
2021	1,001	724,708	3,330	1.4	1,799	1,799
2022	570	412,613	2,290	1.2	1,182	1,182
2023	1,075	778,307	6,490	2.7	3,440	3,440
2024	967	701,846	3,050	1.3	1,671	1,671

Table 7. Summary of flow metrics at the USGS Grand Island (06770500) gage including mean annual value for period of 1958-2024 and annual values from 2009 to 2024.

Water Year	Mean Annual Discharge	Annual Volume (ac-ft)	Mean Daily Peak Discharge	Return Interval (Years)	40-Day Max Discharge	Mean June flow (germination)
1958-2024	1,704	1,234,130	7,197	2.6	3,969	2,791
2009	1,039	752,027	3,430	1.3	2,011	1,337
2010	2,289	1,657,361	8,630	3.5	4,960	5,414
2011	4,214	3,050,551	10,200	5.0	7,982	7,866
2012	978	709,915	3,320	1.2	2,857	372
2013	1,024	741,203	10,100	4.8	3,524	366
2014	1,199	867,919	8,120	3.2	2,778	3,290
2015	3,341	2,418,835	16,000	16.3	12,636	13,370
2016	2,993	2,172,692	8,750	3.6	7,390	6,624
2017	1,585	1,147,311	4,560	1.5	2,943	2,099
2018	1,498	1,084,572	3,010	1.2	2,036	1,450
2019	3,006	2,176,268	18,200	26.0	4,615	3,769
2020	2,005	1,455,474	9,310	4.1	3,755	2,016
2021	1,127	815,662	5,560	1.8	2,437	1,599
2022	613	443,952	2,410	1.1	1,281	1,513
2023	1,116	807,597	6,430	2.2	3,641	3,100
2024	1,073	778,878	3,500	1.3	1,976	1,791

One Extension Science Plan priority is evaluating the effectiveness of releasing flow in June to suppress germination of in-channel vegetation. The Program began germination suppression releases (flow experiments) in 2020 with the objective of maintaining a minimum mean daily discharge at Grand Island for at least 30 days between June 1 and July 15. In 2020 and 2021, the target June discharge was 2,000 cfs at the Grand Island gage and in 2022, the target decreased to 1,500 cfs. **Figure 5** shows mean June flow by year as well as the proportion flow that was attributable to releases from the Environmental Account (EA) in Lake McConaughy.

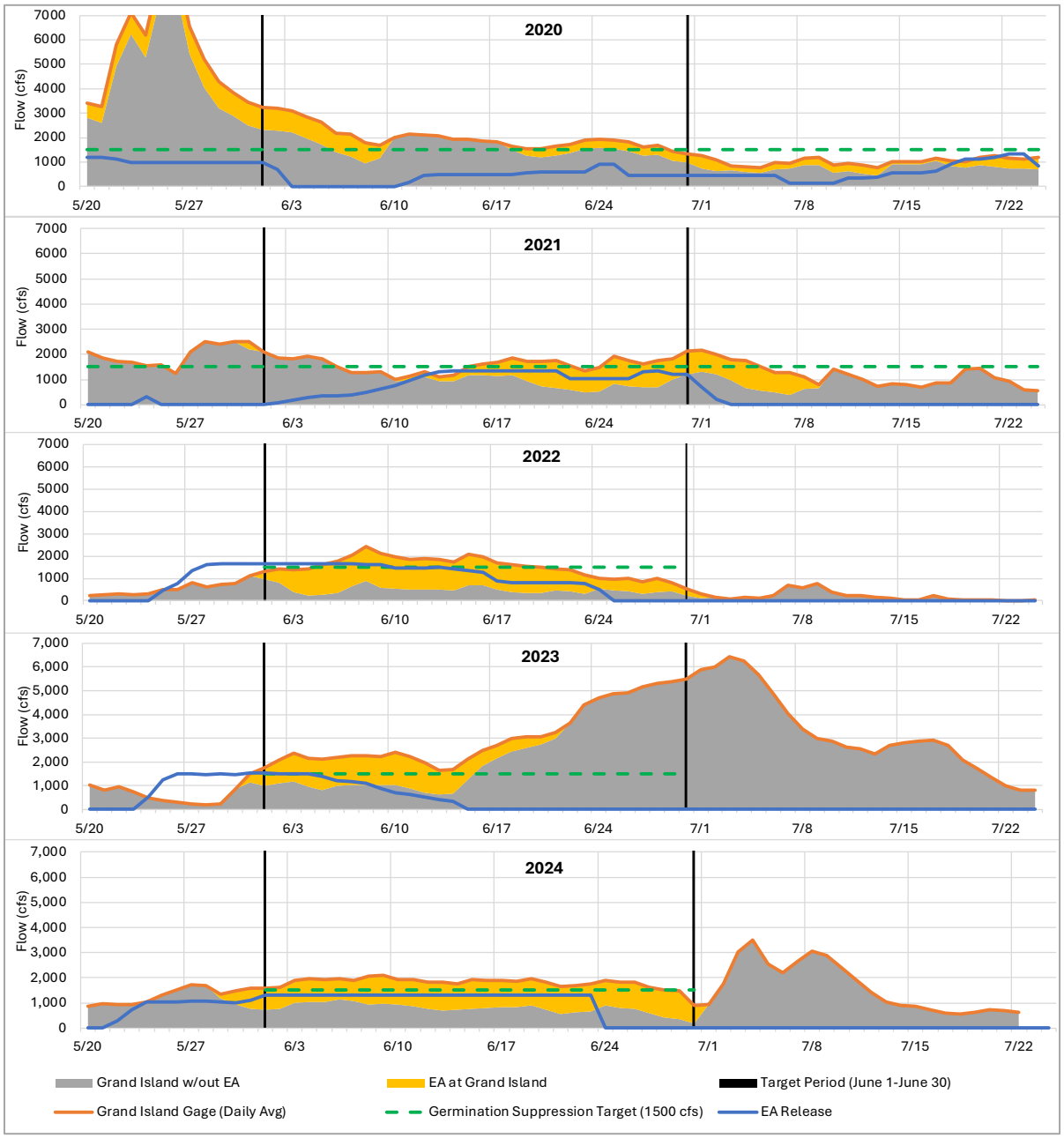

Figure 5. Mean daily discharge (cfs) at USGS Grand Island (06770500) gage (orange) during germination suppression flow release period 2020 – 2024. Figure shows natural flows (grey), releases from the Environmental Account (EA, blue), and the contribution of EA water (gold) toward achieving the current 1,500 cfs release target (green).

In **Figure 6**, the relationship between three hydrologic metrics is illustrated: Mean Daily Peak Discharge (cfs), 40-Day Max Discharge (cfs), and Average June Flow (cfs) representing the germination period from 2007-2024. Mean Daily Peak Discharge shows considerable variability, with notable peaks in 2015 and 2019. The 40-Day Max Discharge and Germination flows generally follow a similar pattern but with smoother fluctuations and lower peak values. Specifically, the 40-day maximum flow in 2019 was much lower than the mean daily peak due to the shorter duration of that natural high flow event. Take special note of the difference in average June flow (germination flow) prior to and after germination suppression releases began in 2020, denoted by the dotted black line. Prior to 2020, average June flow was very low in dry years without natural peak flows (see 2012 and 2013).

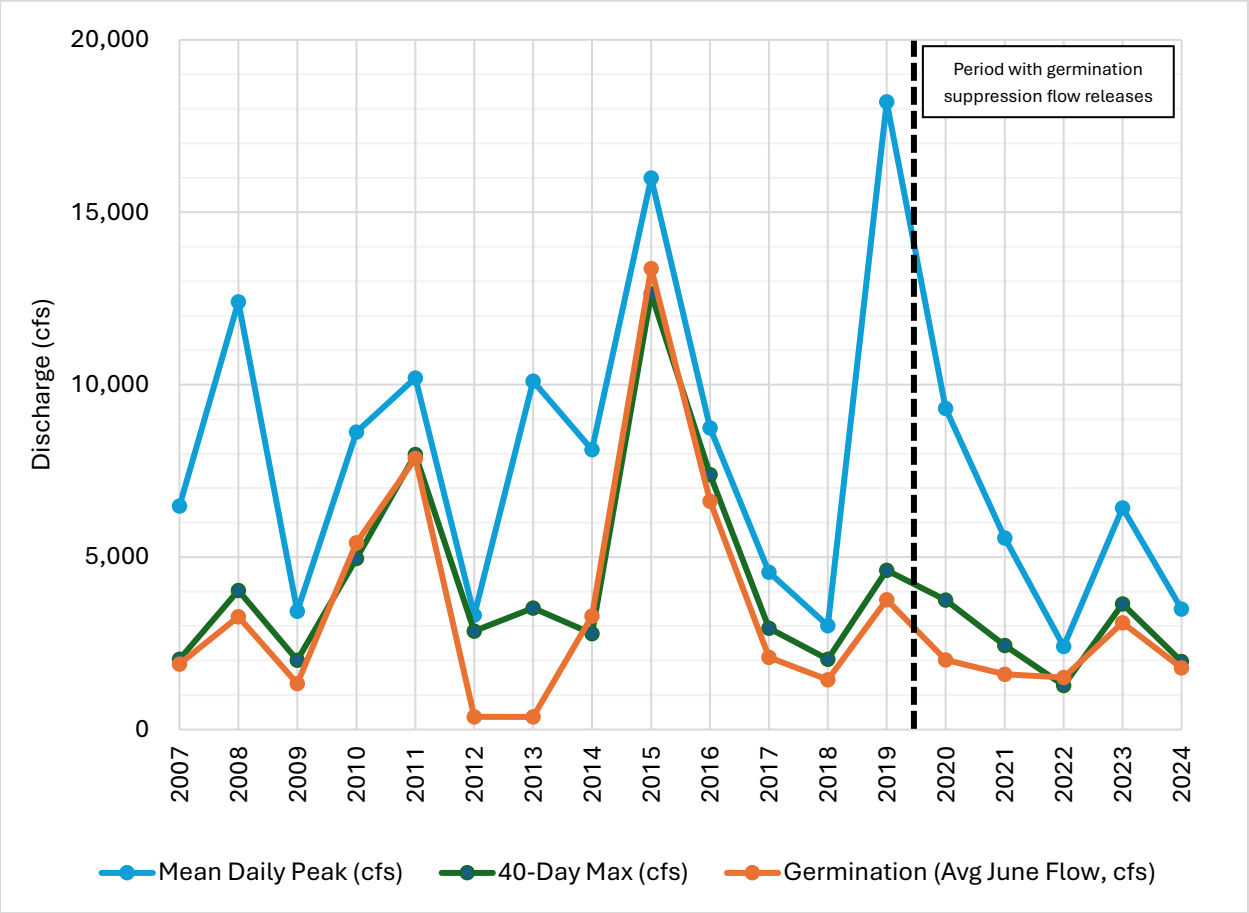

Figure 6. Mean daily peak discharge, 40-day maximum discharge (cfs) and mean June discharge (cfs) at USGS Grand Island (06770500) gage for period of 2007-2024. Beginning of annual germination suppression releases indicated by dashed black line. Note absence of very low June flows after 2020.

Hydrodynamic Modeling

Annual topo-bathymetric data were used to develop annual two-dimensional (2D) HEC-RAS hydraulic models of the AHR that compute depth, velocity, and shear stress at each 2D node over in-channel flows ranging from 500 to 5,000 cubic feet per second (cfs). SRH-2D was previously used to model the AHR and results from this model can be found in the 2020 Geomorphology and Vegetation Monitoring Report (PRRIP, 2022b). A comparison of HEC-RAS and SRH-2D results and capabilities is available in **Appendix A**.

Model results are used to inform four analyses in this report (**Table 8**). First, the 5,000 cfs water extent defines the river channel boundaries and thus the maximum extent of unobstructed channel width measurements. Second, the distribution of flow between main and side channels at 1,500 cfs is used to track changes in the percentage of flow consolidated in the main channel through time. Third, the 1,500 cfs water extent is also used to calculate the wetted widths in the AHR. Fourth, annual changes in area of channel inundated at 5,000 cfs are used to identify lateral erosion.

Table 8. Subset of useful hydrodynamic metrics parameterized from the reach-wide hydrodynamic modeling results

Metric	Utility
Mean wetted width at 1,500 cfs sampled at 1,000 ft transects	Important for assessing relationship between wetted width and vegetation germination
Wetted area at 5,000 cfs	Used to mask in-channel area for clipping total unobstructed channel width and maximum unobstructed channel width
Percent flow consolidated in main channel at 1,500 cfs	Important for assessing relationship between flow and channel width metrics in split flow reaches.
Lateral erosion at 5,000cfs	Used to monitor lateral erosion happening in the channel

Hydrodynamic Modeling Methods

Creating the HEC-RAS Model

To reduce computation time, the hydraulic model is broken into three reaches. The first reach has two upstream boundaries. One on the North Channel at Lexington Bridge, the other at the J2 Return. The reach includes the confluence of these two channels at Overton Bridge and terminates 17,500 feet downstream of Odessa Bridge (including geomorphic reaches 1, 2, and 3B (**Figure 2**). The second reach begins at Odessa bridge and terminates 46,000 feet downstream of the Shelton bridge (including geomorphic reaches 3C, 3d/4a, and 4B), and the third reach begins at Shelton Bridge and terminates 18,000 feet downstream of Chapman Bridge (including geomorphic reaches 4C, 4D, and 5). Small changes in local bed slope can have a large impact on the downstream end of model results. To avoid error due to this local sensitivity, the downstream-most results are discarded where they overlap with the next reach.

Computational meshes for each model were created in HEC-RAS. Topo-bathymetric LiDAR data was converted to a 3ft-by-3ft resolution terrain and a 2D flow area was defined over the terrain. An initial computational node spacing of 25 ft was defined across the entire mesh. Narrow channels, levees, or other areas requiring higher resolution were adjusted using breaklines that were manually drawn. For each new year modeled, breaklines were examined and updated as necessary to reflect changes in channel topography.

The model results used in this report are derived from steady-flow hydrographs that are run for several days to several weeks to reach equilibrium water surface elevations and flows. Normal depth computations are used for all downstream boundary conditions. Slopes for the normal depth boundary are estimated from bed and water surface slope at the downstream end of the reach (**Table 9**).

Manning's Roughness

A single Manning's value was applied throughout each model reach in most cases (**Table 9**). We found this to be appropriate and accurate for our purposes as over-bank flow rarely occurs over the suite of flows simulated for this report. During the calibration process we also determined that the J2 Channel Manning's value should be lower than the rest of the model reach.

Table 9. Reach specific model parameters

Model Reach	Manning's Number	Time Step (min)	# of Upstream Boundaries	Downstream Boundary Slope (ft/ft)
Lexington to Odessa	0.03; 0.028 on J2 Channel	1	2	0.00119
Odessa to Shelton	0.028, increased to 0.03 in 2023	2	1	0.00116
Shelton to Chapman	0.025	1	1	0.00119

Computational Parameters and Process

We used a combination of the Shallow Water Equations (Eulerian-Lagrangian Method) and the Diffusion Wave Equations in model development (HEC, 2022). The shallow water equations (SWE) are more accurate in highly dynamic situations such as the initial wetting of a dry riverbed. For this reason, a procedure was developed where very low river flows of 10 to 20 cfs were run using the SWE equations and then results from these runs were used as the initial conditions for the 500 cfs run. With this procedure the faster Diffusion Wave equations achieved accurate results for 500 to 5,000 cfs runs. We also reduced run-time by using the run from the previous flow as the initial condition for the next higher flow. A time step of 1 to 2 minutes was found to produce stable results for all model reaches (**Table 9**) and further reductions or adjustment of the time step did not change model results.

Calibration and Validation Process

Each of the three model reaches have been calibrated, adjusting Manning's n to better match known water surface elevation data, and validated by comparing model results to measured water

surface elevations. Water surface elevations were measured through field survey or LiDAR each year. Approximately 20 known water surface elevation points were collected each year at various flows and locations along the AHR. Our goal was to capture at least 5 points per reach spread across the main channel and side channels. A USGS gage is located within each model reach at Overton, Kearney, and Grand Island bridges. Gage datums and rating curves were also used to validate model water surface elevations. As shown in **Table 10**, validated models predict water surface elevations with typical average accuracies within one to two tenths of a foot. Larger deviations observed in a single year (such as the Lexington to Odessa reach in 2017) and not as part of a pattern through time are believed to be due more to survey error than model inaccuracy. In each of the cases where average differences exceed a magnitude of 0.3 ft, we found that validation of the reach in question was relying on too few survey points that may have been recorded inaccurately or during a time when hydrocycling caused flow to change rapidly. In response, we have increased our efforts to gather validation data more evenly across the reaches at times when flow is relatively stable. The consistently low average predictions of the Odessa to Shelton model from 2016-2022 led us to increase Manning's n from 0.028 to 0.03 for 2023 modeling, improving accuracy in that reach in 2023 and 2024.

Table 10. Average difference between modeled water-surface elevation and known elevation in feet.

Model Reach	2016	2017	2018	2019	2020	2021	2022	2023	2024
Lexington to Odessa	-0.28	0.49	0.01	0.03	0.06	0.21	-0.19	0.01	0.09
Odessa to Shelton	-0.06	-0.12	-0.14	-0.36	-0.11	-0.17	-0.04	-0.17	0.01
Shelton to Chapman	0.06	-0.03	0.01	-0.09	-0.34	-0.02	0.01	0.05	-0.04

Wetted Width Methods

Wetted widths are calculated to assess the average width of the river at 1,500 cfs. Widths are calculated by clipping 1,000 ft transects to the 1,500 cfs mask created using the hydrodynamic model. The 1,000ft transects are used every year for this analysis, as well as the unvegetated width analysis. The transects were hand delineated to bisect the width of the river through all channels. To assess the river widths, a 5,000 ft moving average is calculated by averaging 5 transect widths by river mile to show width trends and smooth outliers in the data.

Flow Consolidation Methods

Hydrodynamic model results were used to estimate the percentage of total river flow that is consolidated into the main channel[7]. The distribution of flow between main and side channels at flow splits is influenced by channel slope, flow depth, and channel angles at splits. Some of these

[7] The main channel is defined as 1) the channel conveying the majority of flow or 2) channel managed to provide whooping crane habitat in segments like Mormon Island where shifts in flow distribution through time have resulted in side channels carrying more flow than the main channel (**Table 1**, **Figure 2**).

factors vary significantly in depth, meaning that there are limitations to using a 2D (depth averaged) simulation to estimate flow at a split. However, the combination of high-resolution bathymetry data and a typically shallow river suggest that changes in year-to-year modeled flow split ratios will be reasonably accurate.

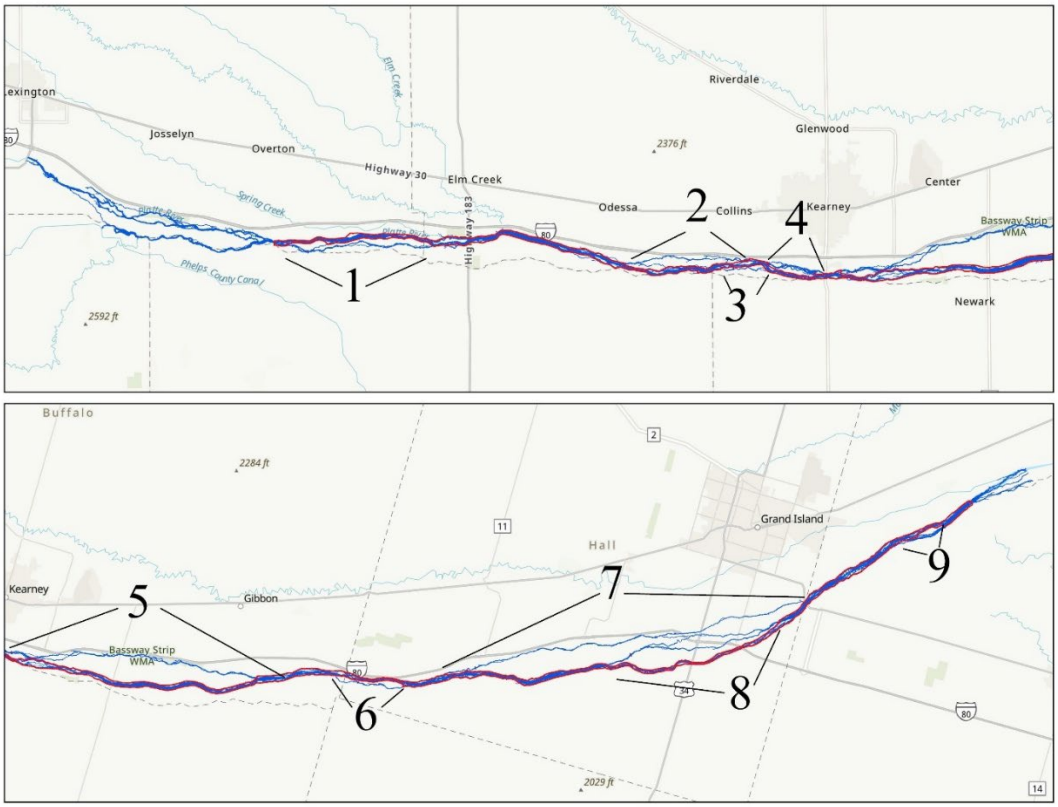

Figure 7. Nine split flow reaches used for flow consolidation analysis.

Nine major split flow segments were visually identified and tracked through time. Flow splits were identified and numbered from 1-9 starting at Overton to Grand Island **(Figure 7)**. The locations of the splits are described by the closest bridge section and whether the flow split is the north or south split. The percentage of flow in main and side channel at 1,500 cfs was calculated from HEC-RAS results for each modeled year[8]. The precise ratio of each flow split changes at flows above or below 1,500 cfs, however, we found that these changes did not alter the overall pattern of findings on these splits. We measured flow splits in RAS Mapper (HEC, 2022) by drawing profile lines perpendicular to side channel flow direction at each split. RAS Mapper interpolates flow across the profile lines from depth and velocity results. Flow in the side channel was then subtracted from total flow to calculate flow in the main channel and percentage of flow consolidated in main channel. In the two instances (Splits 3 and 8) where consolidation was reduced by multiple side channels running in parallel, flow in both side channels was subtracted from total flow to calculate consolidation.

[8] This discharge was used because it is the flow target for the germination suppression flow management action.

Hydrodynamic Modeling Results

Wetted Width

A plot of the 2024 modeled wetted width of all channels at 1,500 cfs (**Figure 8**) shows that width is highly variable throughout the AHR but generally increases in a downstream direction. A plot of the 2024 modeled wetted width of the main channel (**Figure 9**) does not show the same increasing downstream trend because wetted width of the main channel is strongly influenced by the proportion of flow that is consolidated into that channel at any given location along the reach.

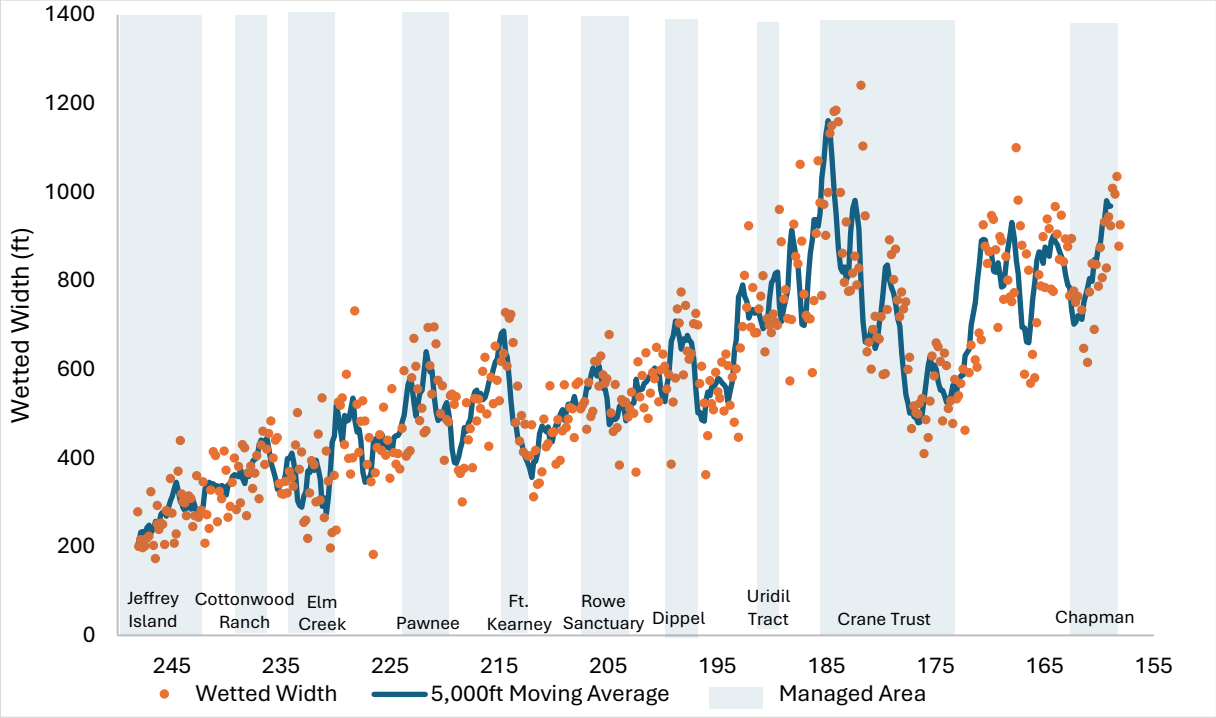

Figure 8. 2024 wetted width of all channels at 1,500 cfs, as sampled at 1,000 ft transect intervals (dots), with a 5,000 ft moving average (blue line), from HEC-RAS hydrodynamic model. Gray bands indicate segments of channel that are managed to improve habitat suitability for whooping cranes.

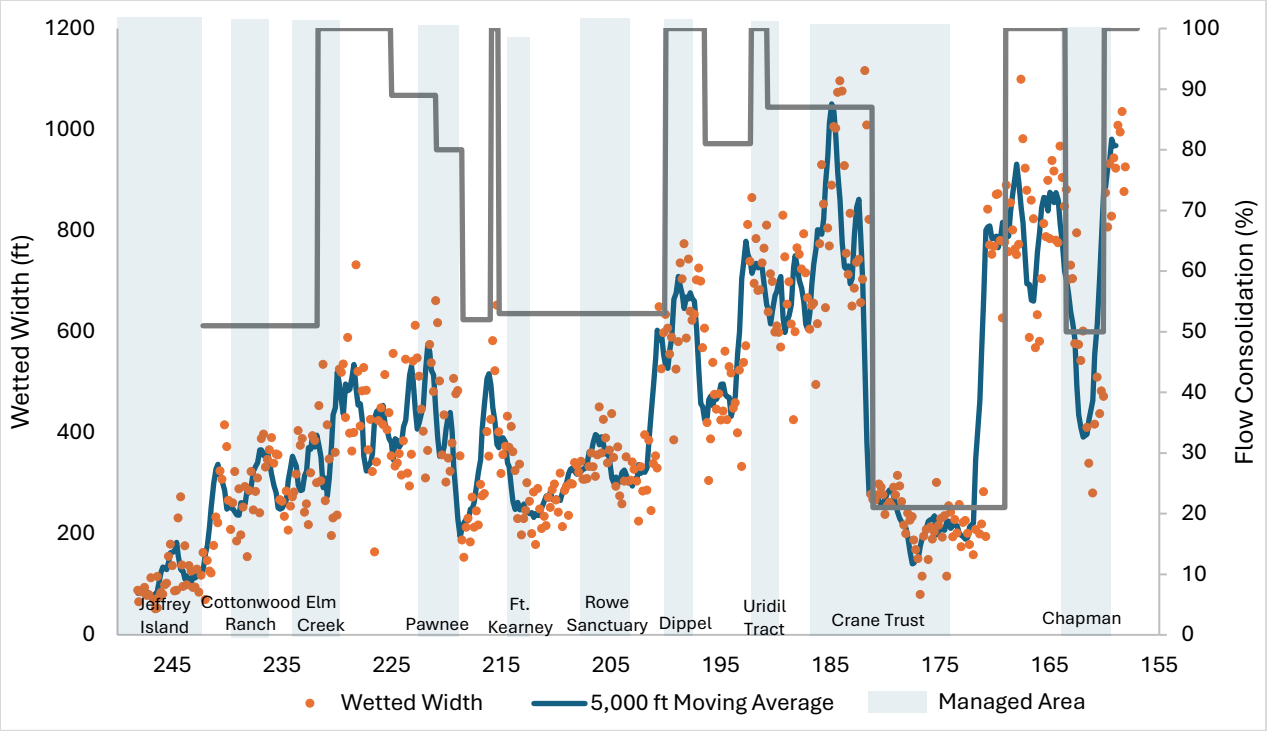

Figure 9. 2024 wetted width of main channel at 1,500 cfs as sampled at 1,000 ft transect intervals (dots), with a 5,000 ft moving average (blue line), from HEC-RAS hydrodynamic model. Gray line indicates percent of flow consolidated in the main channel at 1,500 cfs. Gray bands indicate segments of channel that are managed to improve habitat suitability for whooping cranes.

Comparing wetted width of areas managed to improve whooping crane habitat suitability to unmanaged areas of the main channel provides a cursory indication of the effect of management on channel morphology (**Figures 9 and 10**). Over the entire AHR, the average wetted width of the main channel at 1500 cfs did not change substantially from 2017-2024 (**Figure 10**). Managed areas have on average slightly higher width than other areas for all years besides 2023 and 2024. Reductions in wetted width were most noticeable at the Rowe Sanctuary and Dipple managed properties. However, the differences are small and generally within the bounds of the standard error of the distribution.

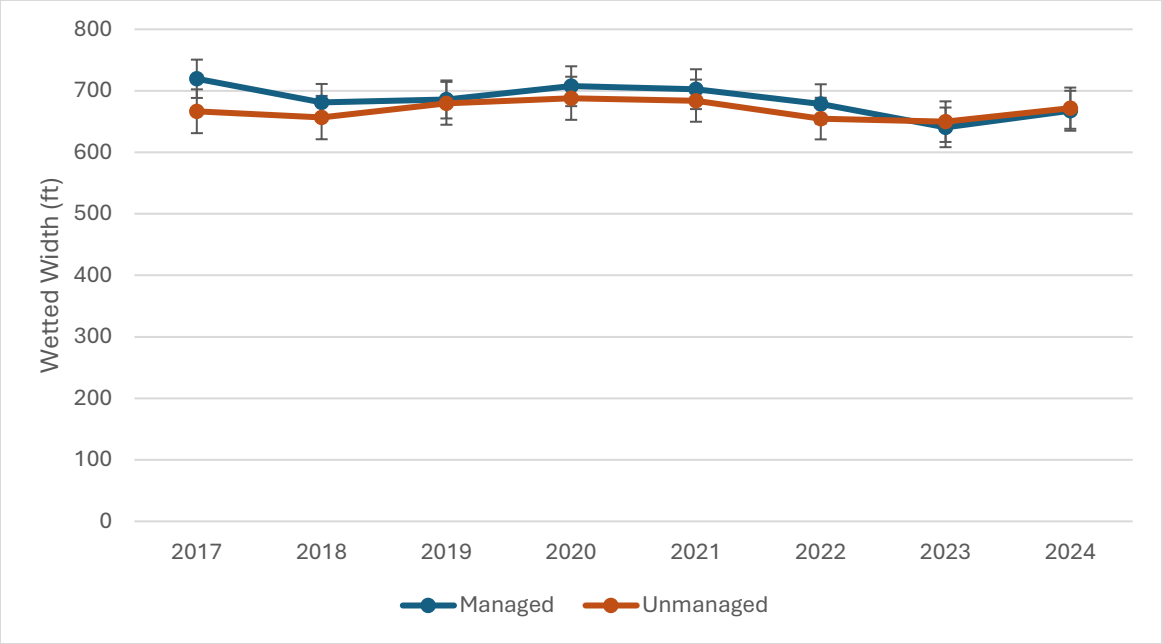

Figure 10. Mean and 95th percent confidence intervals of 1,500 cfs wetted width of the main channel for 2017 to 2024 from Overton to Chapman. Wetted widths are reported separately for segments managed to improve whooping crane habitat suitability and unmanaged segments of the AHR.

Flow Consolidation Results

The percentage of flow consolidated in the main channel through time at 1,500 cfs and general trends by reach are presented in **Tables 11** and **12**.

Table 11. Percent of flow (1,500 cfs) consolidated in main channel (MC) presented by reach upstream to downstream from 2016-2024) along with general trend. Side channel (SC).

#	Location/Description	2016	2017	2018	2019	2020	2021	2022	2023	2024	Trend
1	Overton to Elm Creek; South side channel at Cottonwood Ranch	82%	73%	56%	50%	60%	63%	48%	51%	65%	Reduced Consolidation
2	Odessa to Collins; North side channel, first arc	97%	94%	95%	94%	93%	92%	93%	89%	91%	Small Reduction, MC Dominant
3	Collins to Kearney; South side channel	86%	85%	83%	86%	83%	83%	83%	80%	80%	Small Reduction, MC Dominant
4	Collins to Kearney; North side channel, second arc	30%	30%	39%	42%	47%	44%	47%	52%	47%	Increased Consolidation
5	Kearney to Gibbon; North side channel	38%	43%	50%	57%	53%	53%	57%	53%	54%	Increased Consolidation
6	Denman to Martin; South side channel	93%	89%	82%	79%	81%	81%	81%	81%	86%	Small Reduction, MC Dominant
7	Wood River to Mormon Island; North side channel	86%	85%	84%	79%	85%	87%	85%	87%	85%	No Trend, MC Dominant
8	Mormon Island to Grand Island; Second north side channel	22%	22%	22%	22%	18%	24%	21%	21%	20%	No Trend, SC Dominant
9	Guendel Island; Downstream of Grand Island	49%	60%	55%	57%	60%	60%	54%	50%	48%	No Trend

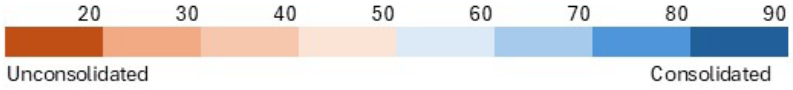

Table 12. Narrative description of flow consolidation in the main channel through time at 1,500 cfs, split flow conditions, and trends.

Flow Split	Description of flow
Split 1 – Overton to Elm Creek	The main channel was fairly consolidated in 2016 with 82% of flow in the that channel. By 2018, however, consolidation fell to 56% and remained low.
Splits 2 and 3	The main channel remained highly consolidated throughout the monitoring period, though there has been a slight decrease over time.
Splits 4 and 5	The main channel carried just 30 and 38% of flow, respectively, in 2016, however this increased to 47% and 54% by 2024. This suggests a trend of increasing consolidation.
Splits 6 and 7	The main channel is dominant. A slight decrease from 93 to 86% was observed at split 6, while no trend was observed over time at split 7. Both were least consolidated in 2019 with 79% flow in the MC.
Split 8	The main channel is highly unconsolidated with only 18 to 22% in the main channel and the rest of the flow going through side channels. No trend was observed over the monitoring period regarding this split.
Split 9	The main channel captured about half of the total flow throughout the monitoring period.

Land Cover Classification

Quantifying land cover change over time is critical for understanding changes in whooping crane habitat suitability as well as measuring the success of mechanical and flow management actions to create and/or maintain suitable habitat. The land cover classes included in this report are water, sand, and vegetation of various height classes. Analyzing trends in coverage of each class can provide essential information about vegetation dynamics in the AHR. From a whooping crane habitat perspective, the most important aspect of classification is defining areas of the channel that provide an unobstructed line of sight (water, sand, or vegetation less than 2 ft in height) or are obstructed by vegetation greater than or equal to 2 ft in height.

Channel width that is unobstructed by tall vegetation is evaluated in two different ways (**Figure 11**). Maximum unobstructed channel width (MUCW) represents the maximum continuous channel width that is unobstructed by vegetation less than 2 ft in height. It is a good predictor of whooping crane roost locations (Baasch et al., 2019). Total unobstructed channel width (TUCW) represents the sum of all segments of channel width unobstructed by vegetation less than 2 ft in height. TUCW is an important physical process metric (Farnsworth et al., 2018) as it is less sensitive to the location of vegetated obstructions within the active channel.

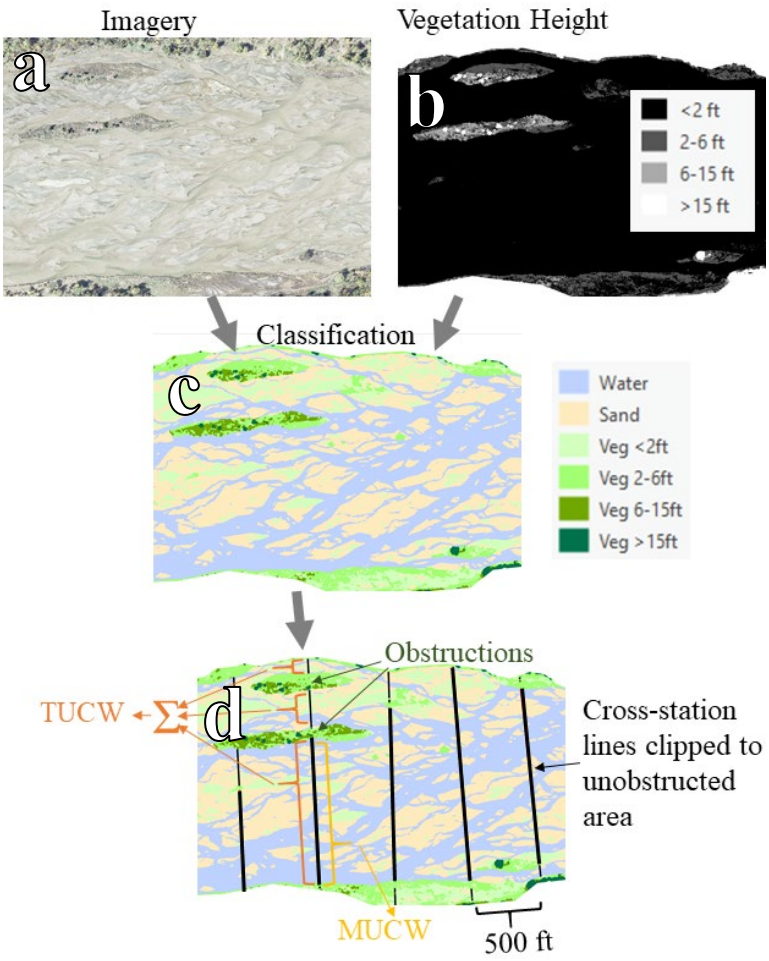

Figure 11. Conceptual diagram illustrates the combination of (a) imagery and (b) LiDAR-derived vegetation height data to (c) classify land cover surface. The land cover surface is then used to (d) clip cross-station lines to unobstructed area, calculate MUCW as maximum continuous channel width that is unobstructed by vegetation ≥ 2 ft in height, and calculate TUCW as the total of all segments of channel width unobstructed by vegetation ≥ 2 ft in height.

Land Cover Classification Methods

Object-based classification is an automated algorithmic method that can interpret remote sensing data, categorizing it into predefined land cover classes. The Program conducts object-based classification of land cover class using the aerial imagery and LiDAR collected in the fall of each year. This algorithmic methodology replaced the visual classification method that was used from 2009 to 2016. The 2020 system-scale monitoring report (PRRIP 2022b) includes a comparison of results using both methodologies and rationale for switching to an object-based classification methodology.

Data Collection and Model Building

The remote sensing data used for classification was collected via airplane by NV5 (previously known as QSI) in either October or November from 2017-2024. NV5 processed the data into

coverages including 4-band (red, green, blue, and near-infrared) imagery and LiDAR elevation surfaces including (in part) topo-bathymetric bare earth and the top of vegetation that were used in this analysis to calculate vegetation height. NV5 assessed accuracy for each year of data collection using ground control check points (QSI, 2016; QSI, 2017; QSI, 2018; QSI, 2019; QSI, 2020, NV5, 2021; NV5, 2022; NV5, 2023; NV5, 2024). The elevation vertical accuracy, presented here as a 95% confidence interval for elevation estimates, varied from 0.1 to 0.2 ft between years on dry, unvegetated surfaces.

Object-based classification was conducted using Trimble eCognition software (Trimble, 2021). In object-based classification, pixels are grouped into spectrally homogenous objects, and then the objects are classified utilizing user-defined criteria. This method differs from the more traditional pixel-based classification, in which all pixels are classified by their individual spectra (Burnett & Blaschke, 2003). Object-based classification has been demonstrated to be more effective than pixel-based classification in a wide variety of environments (Blaschke, 2010), and a powerful tool for specifically classifying patches of in-channel vegetation on sandbars (Demarchi et al., 2016).

The land cover classification schema incorporated six classes as defined in **Table 13**. Both the imagery and elevation data were classified at 3 ft spatial resolution. Water and sand were differentiated from vegetation using the Normalized Difference Water Index (NDWI) and Normalized Difference Vegetation Index (NDVI). NDWI and NDVI are indices combining reflectance in the green and near-infrared bands (McFeeters, 1996), and the red and near-infrared bands (Rouse et al., 1973), respectively. NDVI values range from -1 to 1 and are positively correlated with leaf density and health (Rouse et al., 1973). NDWI values also range from -1 to 1, with positive values representing water (McFeeters, 1996).

Table 13. Land cover classes derived from object-based classification, obstructed or unobstructed classification, and typical vegetation type.

Land Cover Class	Obstructed/Unobstructed	Typical Vegetation Class
Sand	Unobstructed	Unvegetated
Water	Unobstructed	Unvegetated
Vegetation < 2ft	Unobstructed	Sparse or dense short herbaceous
Vegetation 2 - 6 ft	Obstructed	Tall herbaceous or *Phragmities*
Vegetation 6 - 15 ft	Obstructed	*Phragmities* or woody vegetation
Vegetation > 15 ft	Obstructed	Woody vegetation

Water was differentiated from land using the NDWI and sand was differentiated from short vegetation using NDVI. The cutoff values for both indexes were visually calibrated for each year—values are presented in **Table 14**. Annual NDVI calibration is necessary due to the impact of climactic variations on vegetation health. Vegetation was then differentiated into height classes using the LiDAR vegetation height surface (**Figure 11b**). This process generated a reach-wide map of land cover classes as shown in **Figure 11c**. In-channel land cover classes less than 2ft in height were considered unobstructed (sand, water, vegetation less than 2ft), that is, they were not considered as presenting a visual obstruction to whooping crane utilizing the channel.

Table 14. NDWI and NDVI cutoff values for 1) separation of water and terrestrial and 2) separation of sand vs. vegetation, respectively. Values were visually calibrated for each year.

eCognition Year	NDWI Value	NDVI Value
2017	0.01	0.07
2018	0.01	0.07
2019	0.01	0.07
2020	0.05	0.06
2021	0.01	0.08
2022	0.09	0.07
2023	0.01	0.06
2024	0.01	0.07

Validation Methods

Classification analyses were validated by comparing object-based classification results to field data. For best comparison, field validation points were collected within a week of the imagery collection flight. Field data were also collected in 2017 but were not used because the classification schema did not have clear mapping to our current vegetation classes. These field values did not have height classifications and therefore could not be used to distinguish between obstructed vs unobstructed vegetation classes.

The comparison analysis indicated obstructed / unobstructed area agreement exceeded 80% in six out of seven years and 90% in three out of seven years. Agreement in classification of obstructed vs. unobstructed areas was low, at 70%, in 2022 due to portions of the acquired imagery covered with ice that interfered with the classification (**Table 15**). The most common error was classification of points identified in the field as tall vegetation (greater than 2 ft) and some classified as shorter class of vegetation. This error is a result of the spatial scale of the remote sensing data. The vegetation height rasters used in analysis represent the average elevation of the LiDAR point cloud within each 3 ft x 3 ft cell. If a vegetation patch is small or sparse, the highest points may average to a lower value at the point of conversion from LiDAR point cloud to raster. During the modeling process, we implemented a rule ensures there is minimum of 4 pixels to create a patch of that classification. This helps to prevent breaks in the water from logs or debris, but this can also create error if there are small patches of one height class within another class. For example, a cell that contains a sparse or partial patch (< 4 pixels) of vegetation within it that is 2.5 ft in height will be absorbed into the predominant surrounding height class which may have an average elevation value lower than 2 ft. The small error or disagreement that occurs in differentiating between obstructed and unobstructed points is largely due to this error.

Table 15. Results of eCognition classification agreement to validation points by year.

Year	Total Classification Agreement	Percent of Disagreement Attributable to Vegetation Height	Obstructed/ Unobstructed Agreement	Disagreement between Obstructed/Unobstructed Incorrectly Classified as Unobstructed	Number of Validation Points
2018	75%	6%	91%	66%	401
2019	66%	12%	84%	97%	187
2020	81%	6%	97%	0%	115
2021	71%	24%	81%	100%	442
2022*	53%	45%	70%	100%	278
2023	77%	13%	91%	100%	177
2024	76%	3%	95%	90%	184

* Ice in aerial imagery interfered with the classification.

Unvegetated Width Calculations

Land cover classification maps were used to identify the total area of each class and to calculate MUCW and TUCW (**Figure 11d and Table 16**). MUCW and TUCW were extracted by spatially clipping cross-station lines spaced at 1000 ft intervals throughout the AHR to the area of unobstructed classes—water, sand, and vegetation less than 2 ft in height (**Figure 11d**). TUCW and MUCW were additionally clipped to the 5,000 cfs flow extent to prevent unvegetated line segments from extending overbank. MUCW was then measured at each of the clipped cross-station lines as the maximum continuous channel width that is unobstructed by vegetation less than 2 ft in height. TUCW was measured at each of the clipped cross-station lines as the total of all segments of channel width unobstructed by vegetation less than 2 ft in height.

MUCW and TUCW of transects were calculated using hand delineated 1,000ft spaced transects that bisect the width of the river through all channels of the Platte across the AHR. MUCW and TUCW are calculated by clipping the transects to the unobstructed eCognition classes – water, sand, and vegetation less than 2ft. For maximum unvegetated channel width, the longest segment of the clipped transect is used and for total unvegetated channel width, the entire length of the transect is calculated (**Figure 11d**). A 5,000 ft moving average is calculated for both MUCW and TUCW by averaging five transect widths by river mile to show width trends and smooth outliers in the data.

Table 16. In-channel habitat metrics derived from land cover classifications that are important for whooping cranes.

Metric	Metric Symbol	Definitions
Maximum Unobstructed Channel Width	MUCW	The longest continuous channel width unobstructed by vegetation ≥ 2 feet in height
Total Unobstructed Channel Width	TUCW	Sum of all segments of channel width unobstructed by vegetation ≥ 2 feet in height
Percent Unobstructed Area		Percent area of the channel unobstructed by vegetation ≥ 2 feet in height

Land Cover Classification Results

To assess the change in habitat classes, the land cover in the 5,000 cfs mask was calculated by year. In **Figure 12**, you will see the total acres of land cover in each class for that year. The total area calculated is different every year because the 5,000 cfs mask, which changes annually, is used to clip the area of interest. We wanted to look at the area in the 5,000 cfs mask because this area is the most impacted by river flow. It is important to look at change in vegetation classes within this mask. It is also important to note that while looking at raw acreage values, the sum each year is not the same. This also impacts the percentage of change shown in **Tables 17 and 18**, specifically in the Veg 6 to 15ft and Veg greater than 15ft categories. Sometimes changes here could be due to the 5,000 ft mask getting larger and encompassing more of these tall vegetation classes, rather than vegetation growing taller. **Tables 17 and 18** show the raw acreage values by year for each land cover class and the percentage change by year. Summing raw acreage across all land cover classes produces the total 5,000 cfs mask area each year.

The total area of unobstructed channel - water, sand, and vegetation less than 2 ft in height has stayed within a 2% difference in change from 2017 to 2023. In 2024, unobstructed classes decreased by 5%. Obstructed channel area decreased in 2019 by 59%, likely due to the high flow events that occurred that year. Most of that decrease was due to a reduction in vegetation 2 to 6 ft in height, which decreased by 67%, but vegetation greater than 6ft in height also decreased. We infer that the decrease in obstructed area in 2019 was driven by lateral erosion of higher islands and banks with tall, established vegetation.

In 2020, the coverage of vegetation 2 to 6 ft in height increased by 192%, to encompass more area than was observed in 2017-2019. Water, sand, and vegetation less than 2 ft in height simultaneously decreased in coverage, suggesting that vegetation on islands and near-overbank areas recovered quickly from the 2019 flood disturbance. The imagery in 2022 has ice present in the water which likely resulted in an over classification of ice as sand and not as vegetation less than 2ft. You can see there is a 100% reduction from 2021 to 2022 in vegetation less than 2ft. This class increases again in 2023 when there is no ice present in the channel. In 2024, vegetation less than 2ft category is lower, but all obstructed vegetation classes are higher for this year. When comparing this increase in 2024 to **Figure 15**, there is a decrease in MUCW and TUCW, due to an increase in obstructed vegetation class area.

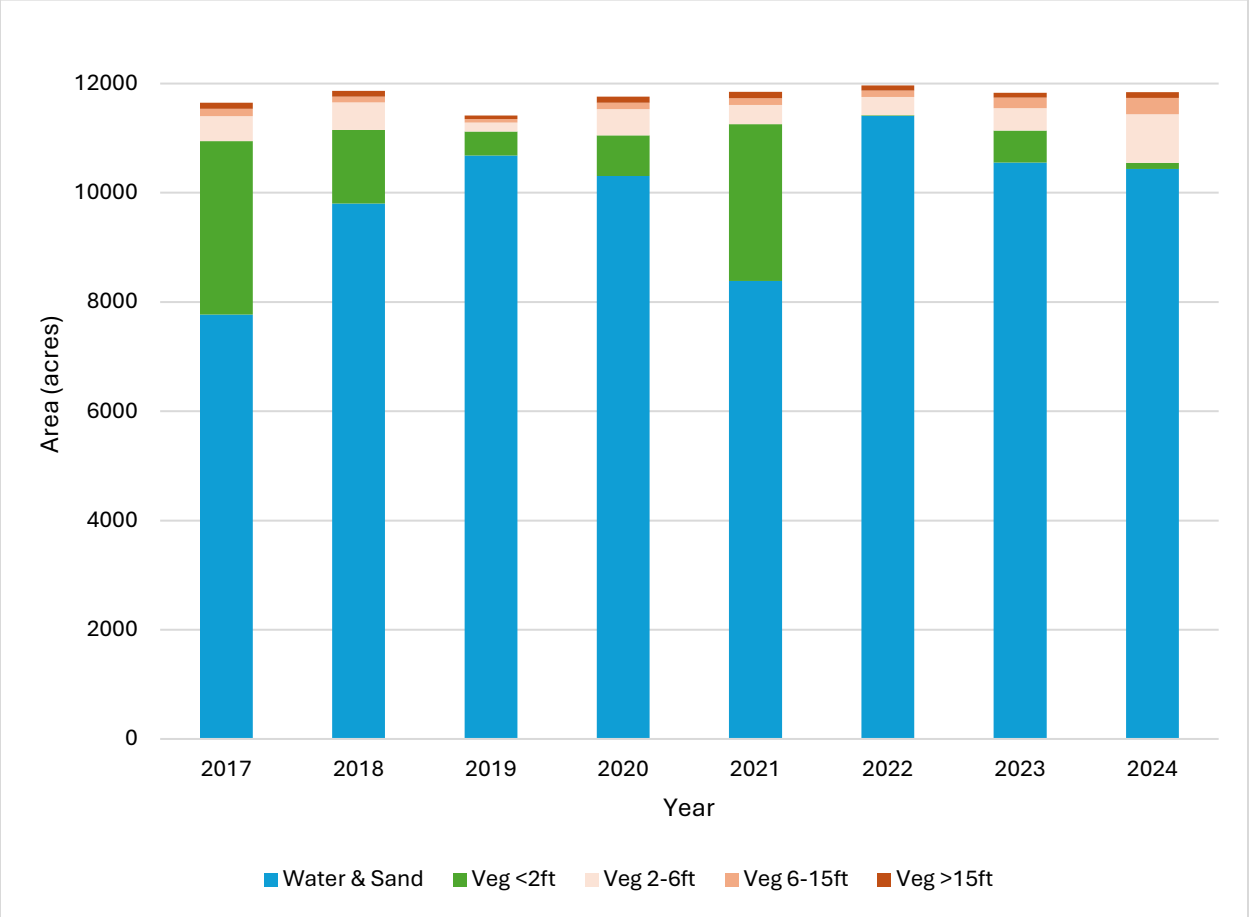

Figure 12. Total area in acres occupied by each land cover class in the main channel, 2017 - 2024. Blue and Green bars are unobstructed categories and shades of red bars are obstructed categories.

Table 17. Area and percent change of all classes measured in each year in the main channel from 2017 - 2024. Negative percent change is denoted by values in parentheses.

	Class	Water & Sand	Veg <2ft	Veg 2-6ft	Veg 6-15ft	Veg >15ft
Area (acres)	2017	7770	3175	456	138	111
	2018	9804	1350	501	105	106
	2019	10682	441	164	63	66
	2020	10307	747	479	119	111
	2021	8383	2872	352	122	119
	2022	11411	12	332	117	93
	2023	10551	587	409	196	88
	2024	10437	113	888	298	107
Percent Change	2017-2018	26	(57)	10	(24)	(5)
	2018-2019	9	(67)	(67)	(40)	(38)
	2019-2020	(4)	69	192	87	70
	2020-2021	(19)	284	(27)	3	7
	2021-2022	36	(100)	(5)	(4)	(22)
	2022-2023	(8)	4,755	23	68	(6)
	2023-2024	(1)	(81)	117	52	21

Table 18. Area and percent change of obstructed and unobstructed main channel area in each year from 2017 - 2024. Negative percent change is denoted by values in parentheses.

	Class	Unobstructed	Obstructed
Area (acres)	2017	10945	705
	2018	11154	712
	2019	11123	293
	2020	11054	709
	2021	11255	593
	2022	11423	543
	2023	11139	693
	2024	10550	1293
Percent Change	2017-2018	2	1
	2018-2019	(0)	(59)
	2019-2020	(1)	142
	2020-2021	2	(16)
	2021-2022	1	(8)
	2022-2023	(2)	28
	2023-2024	(5)	86

When 2024 MUCW and TUCW in the main channel are plotted by river mile (**Figures 13 and 14**), they exhibit a high degree of variability. These plots show the width (in feet) of transects spaced 1,000 ft apart and the 5,000 ft moving average by river mile to smooth the trend. MUCW is more variable than TUCW due to its higher sensitivity to the location of obstruction within the channel.

Small in-channel obstructions can reduce MUCW by hundreds of feet, cutting it in half or more, while impacting TUCW only minimally. In these figures, you can see how flow consolidation can have an impact on unvegetated widths. If you look at river mile 180 to 167, you can see the flow in the main channel is around 20% consolidated and unvegetated widths are much smaller than the surrounding river areas.

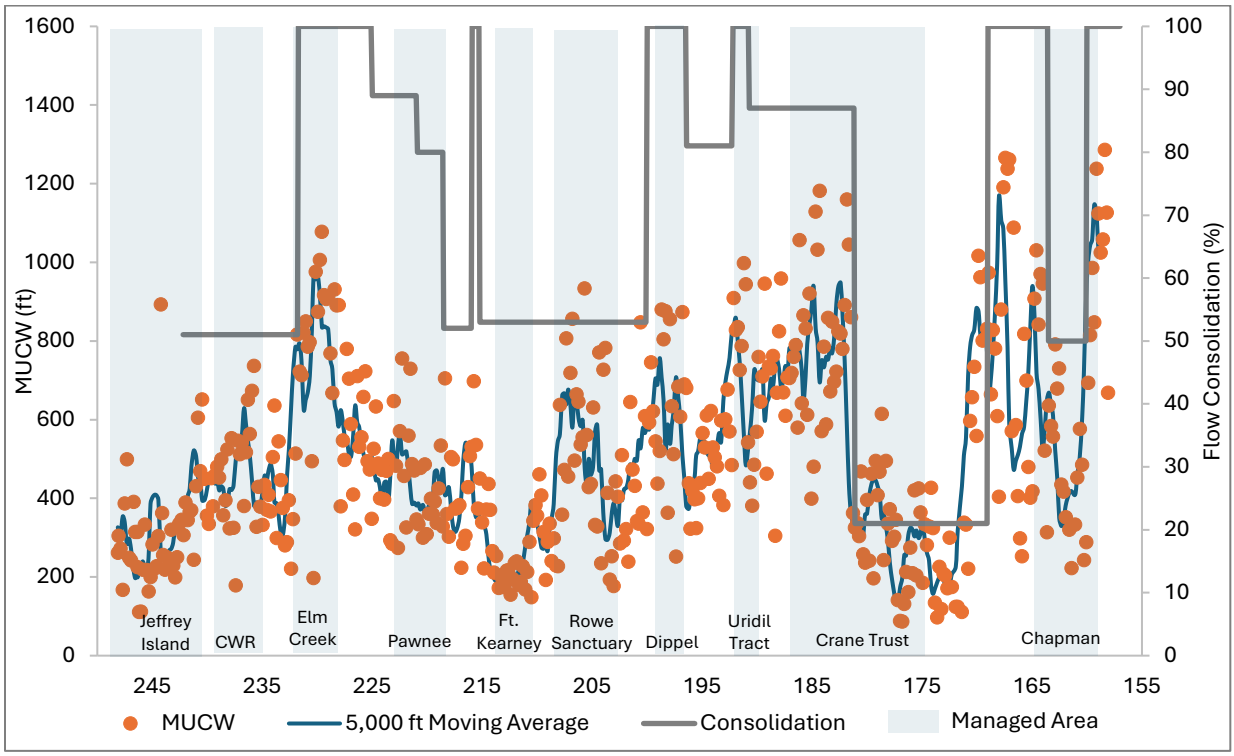

Figure 13. 2024 maximum unobstructed width (MUCW) of main channel, as sampled at transects spaced at 1,000 ft intervals (dots), with a 5,000 ft moving average (blue line). Channel areas managed to create or maintain suitable whooping crane habitat are shaded blue. Flow consolidation in the main channel is shown as a gray line that ranges from 100% consolidated to 20% consolidated.

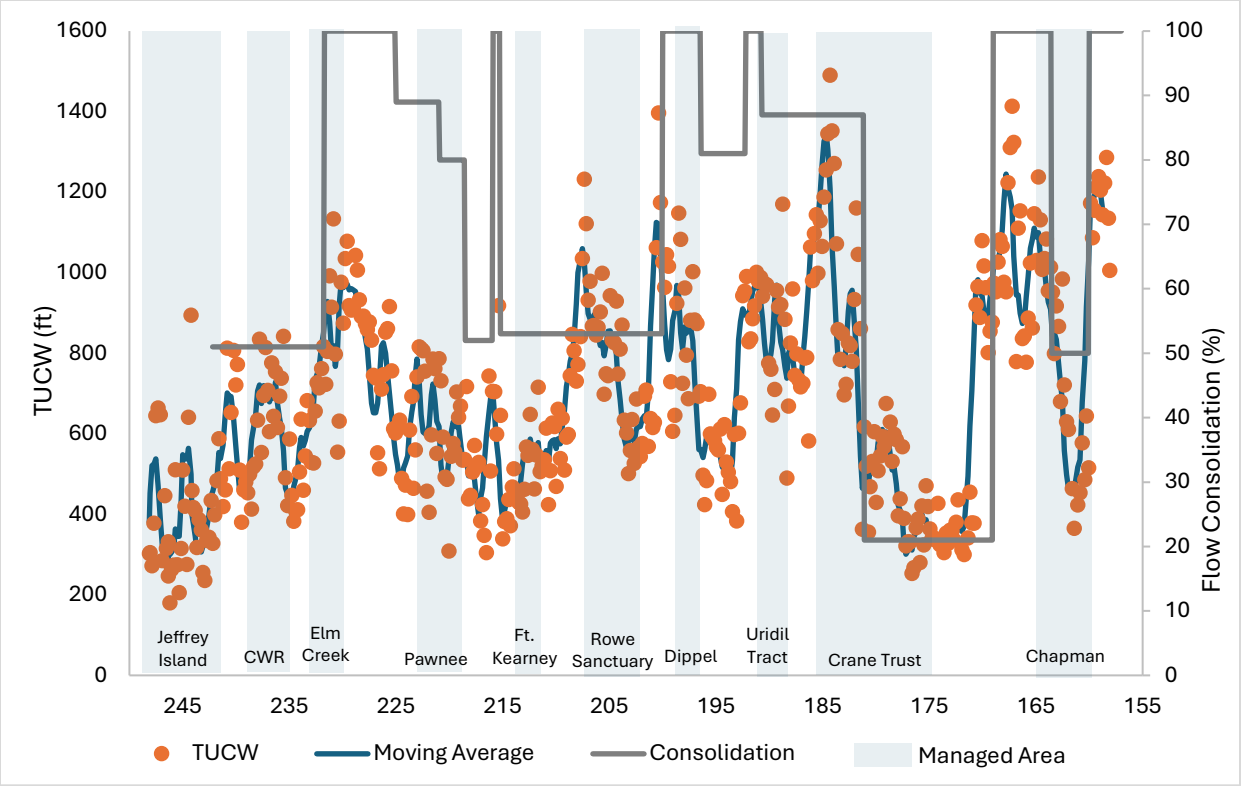

Figure 14. 2024 total unobstructed width (TUCW) of main channel, as sampled at 1,000 ft transects (dots), with a 5,000 ft moving average (blue line). Channel areas managed to create or maintain suitable whooping crane habitat are shaded blue. Flow consolidation in the main channel is shown as a gray line that ranges from 100% consolidated to 20% consolidated.

MUCW and TUCW for the main channel were calculated for the period of 2007-2024 using two methods (**Figure 15**). From 2007 – 2016, unvegetated channel widths were estimated in the field at anchor point locations as well as visually identifying vegetation using aerial imagery (Farnsworth et al., 2018). From 2017 to 2024, a remote sensing based approach (described above) was used to calculate MUCW and TUCW. For a comparison between the two approaches, see Continuity With Older Data section in the 2020 Geomorphology and Vegetation Report (PRRIP, 2022b). In **Figure 15**, TUCW increased in 2015 following a peak flow event. Following peak flow events in 2008, 2011, and 2019, there were less substantial TUCW width responses. In the last seven years, between 2017 and 2024, when remote sensing-based methods were used, MUCW and TUCW had minor fluctuations. During this time MUCW stayed consistent with an average of 530 ft width over all years, and a range of 491 ft in 2017 to a peak of 559 ft in 2022 (**Figure 15**). TUCW was more consistent from 2017 to 2024 with an average TUCW for all years of 714 ft and a range of 689 ft in 2024 to 734 ft in 2017. In **Figure 16,** you can see a dip in the average managed MUCW below the unmanaged MUCW. Reductions in unobstructed channel widths in managed areas were most noticeable in Rowe Sanctuary and Dippel properties.

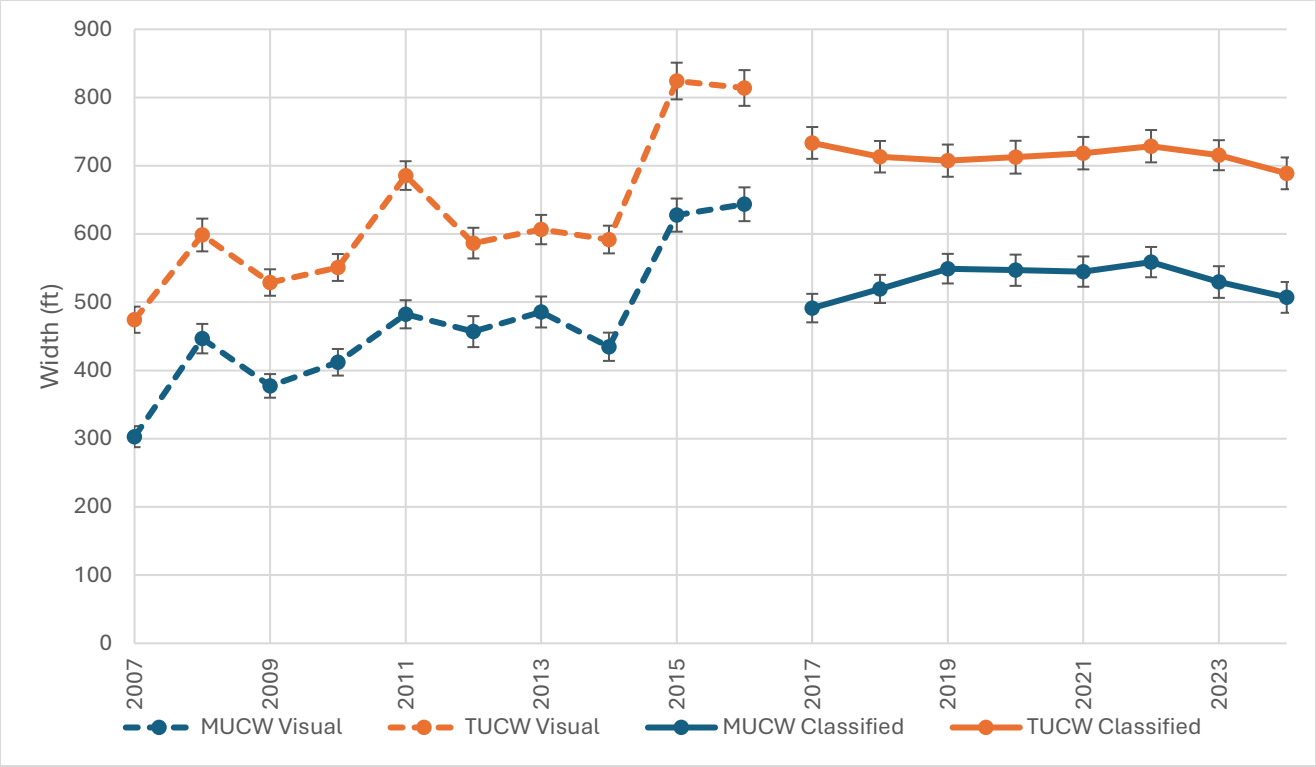

Figure 15. MUCW and TUCW average in the main channel by year measured at 1,000ft transects. Note the visual classification in a dotted line and remote sensing classification in a solid line.

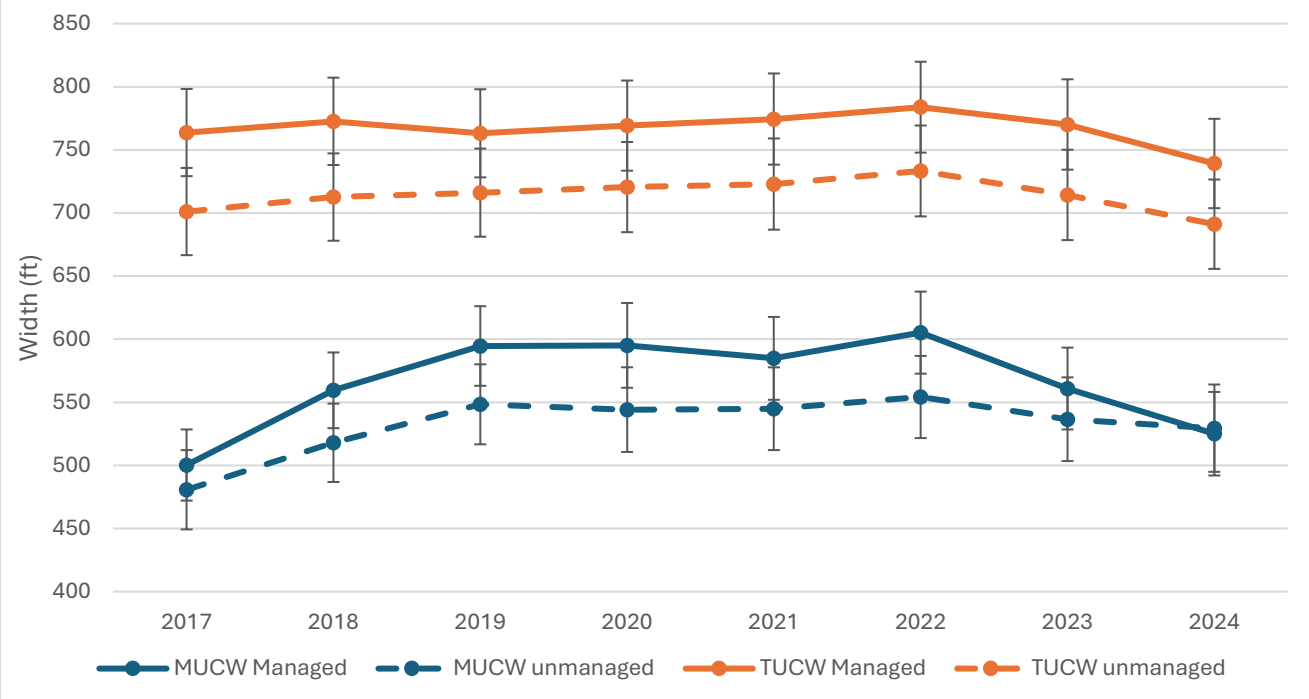

Figure 16. Mean of MUCW and TUCW for main channel areas from Overton to Grand Island. The plot is divided by areas managed to reduce in-channel vegetation (solid line) and those that are not managed (dotted line).

Ongoing PRRIP research has indicated that mean daily peak (Q_P), 40-Day Max ($Q_{MAX\,40}$), and mean discharge during the seed germination period in June (Q_{June}) may influence the occurrence and distribution of in-channel vegetation in the AHR. These metrics are plotted together in **Figure 17** with TUCW estimated from visual classification from 2007-2016 and object-based classification from 2017-2024. As demonstrated in the figure, TUCW increased substantially in 2015, following a peak flow event with both high magnitude (Q_P) and duration ($Q_{MAX\,40}$). Smaller channel width increases occurred following 2008 and 2011 peak flow events. TUCW remained stable during the period of 2017-2024 despite years with no substantial peak flow. During those years, germination season flow was higher than during prior drought years (2012-2013) indicating that channel inundation during the germination season may be preventing vegetation from establishing in the channel.

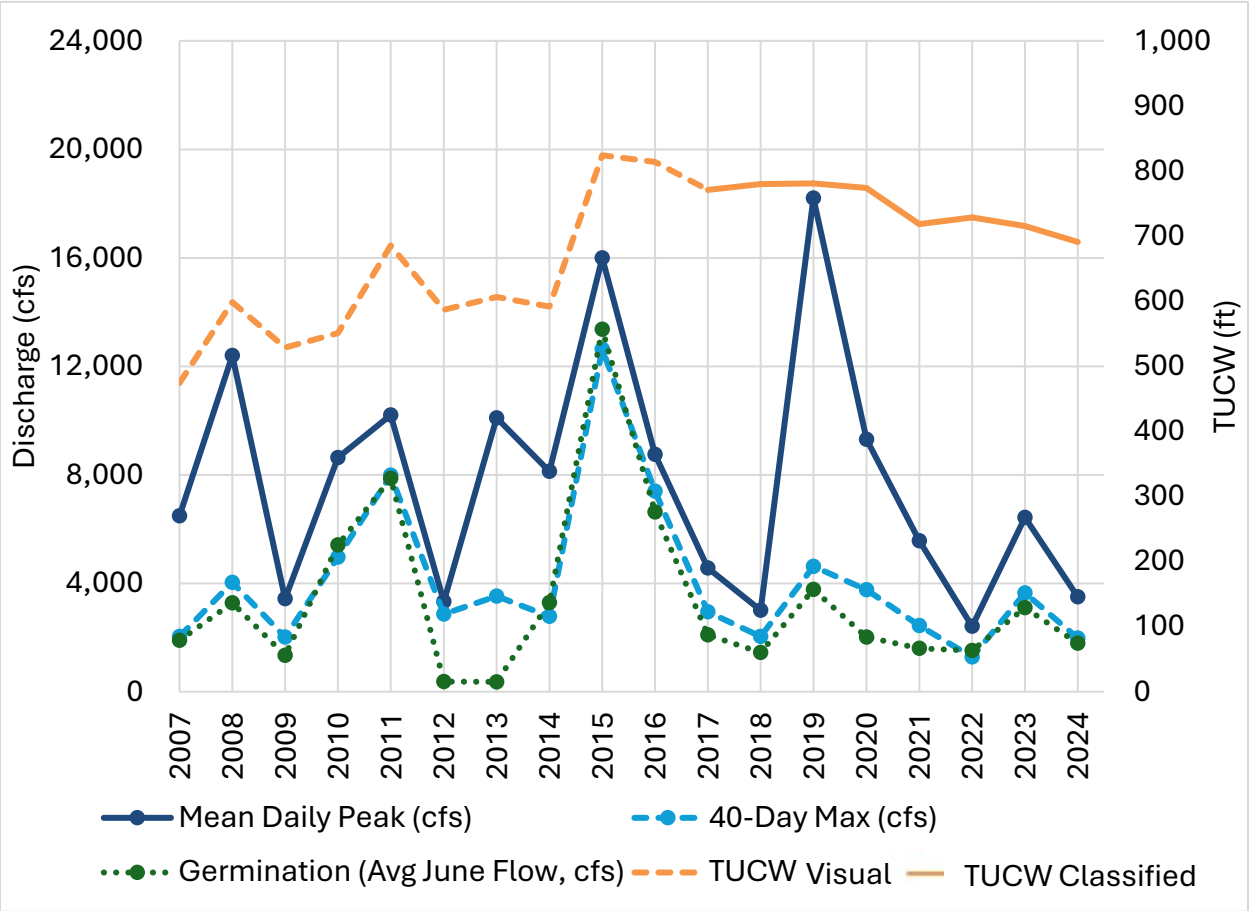

Figure 17. Hydrologic metrics and corresponding main channel TUCW as measured with visual classification from 2007 to 2016 and object-based classification from 2017-2024.

Volume Change Analysis

Quantifying annual variation in sediment volume is critical for understanding changes in channel morphology and habitat in the AHR and for evaluating the success of management actions. This analysis helps to monitor sediment flux, degradation, and aggradation throughout the AHR using repeat LiDAR data and hydraulic modeling. A negative sediment balance resulting in a degradational channel has been identified as one of the primary drivers of historic habitat loss for PRRIP target species (DOI, 2006).

Volume Change Methods

LiDAR Raster Differencing

Annual volume change estimates were developed via LiDAR DEM differencing. We created annual DEMs of difference (DoDs) by subtracting the earlier year from the more recent year (i.e. 2017 – 2016). Each pixel value of the DoD represents the change in elevation (in ft) that occurred in that area. Multiplying these values over the raster cell area (9 ft^2) produces an estimate of volume change in that area. Volume change can then be summed to obtain cumulative change over areas of interest.

AggDeg and Lateral Erosion Mask Creation

We found it is important to set limits to volume analysis that exclude areas outside the active channel as much as possible (PRRIP 2024). Doing so eliminates non-random error in LiDAR data that occurs over floodplain areas due to year-to-year changes in vegetation. For example, bare earth elevation in a meadow in a year when it is not hayed and has high levels of thatch will often be slightly higher than the same meadow in a year when it is hayed. This systematic error is usually only a few tenths of a foot in magnitude but transformed to a volume and propagated over a large field it has the capacity to introduce noise into the volume change results.

To calculate volume change over the active channel only, a polygon mask was created for each DoD. The mask is based on the wetted area of the largest in-bank flow simulated with the hydrodynamic model (5000 cfs). The wetted area is simplified by removing channels less than 15 feet wide and buffered to include channel banks.

To separate bed aggradation and degradation changes from lateral erosion, we created a second series of masks for each DoD that approximate areas of change due to lateral erosion. We defined lateral erosion as areas that experienced bank erosion or failure due to hydraulic activity. Following this erosion, previously dry areas become accessible to flow. To identify these “newly wet” areas and thus areas of lateral erosion, we converted HEC-RAS modeled water extents into 3x3 ft water surface elevation raster grids (**Figure 18A**). We then intersected the raster data (2,500 cfs in the J2 Return Channel and 5,000 cfs below the North Channel confluence) and identified cells where water was newly present to create a mask of lateral erosion for each difference raster (**Figure 18B**). Note that with this method sediment augmentation projects from 2017 to 2022 get counted as well. Volume mechanically removed from banks and placed on the channel bed is categorized at lateral erosion and bed aggradation, the same as if this process occurred due to natural bank failure.

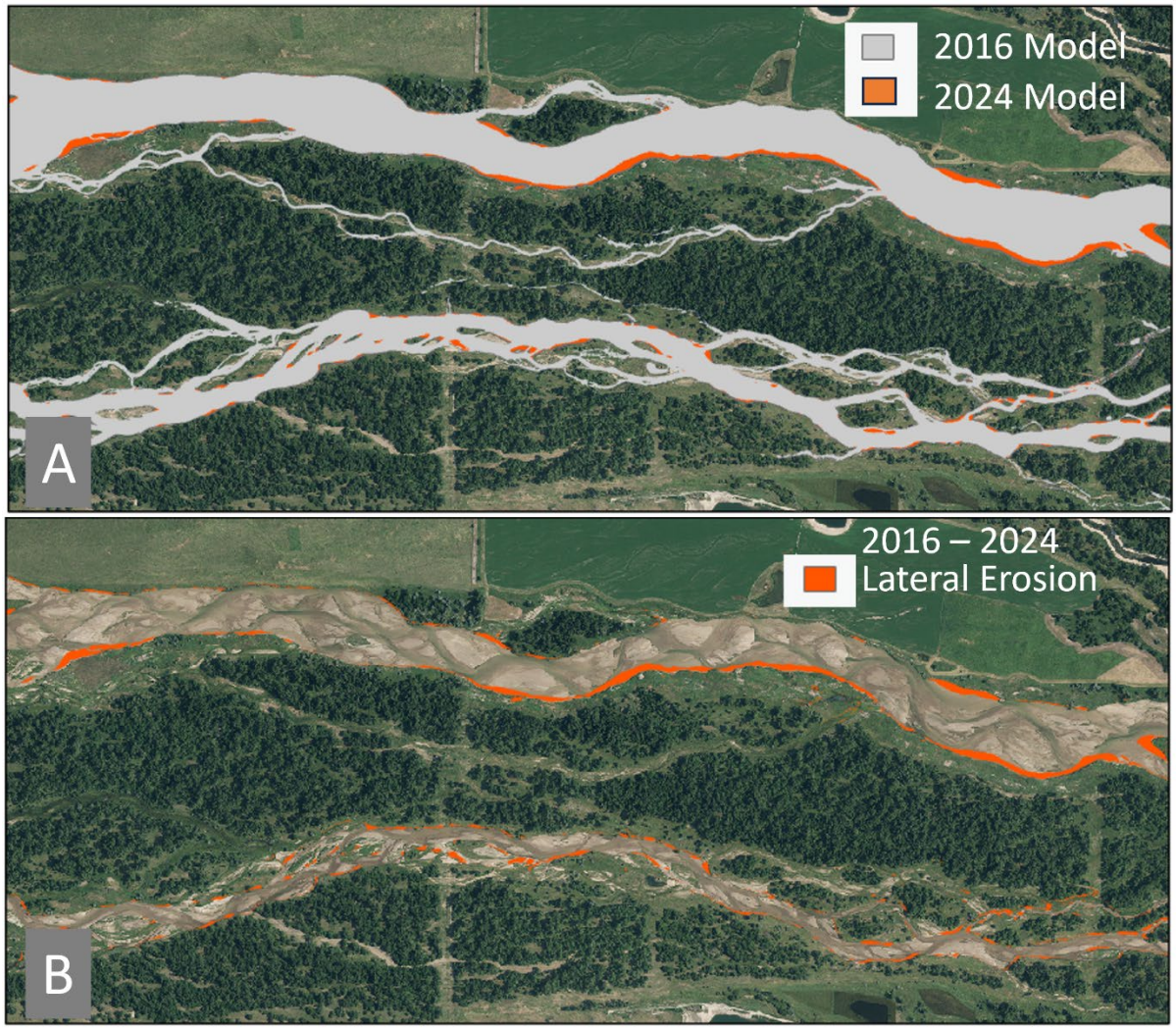

Figure 18. Lateral erosion was delineated by (A) differencing hydraulic model results and (B) isolating newly wet areas.

Reaches

Volume change results for this report are summed at a geomorphic reach scale. The geomorphic reaches are shown in **Figure 19.** Reaches vary in slope, width, and consolidation. Some reaches are composed of a single wide channel, while others contain many channels separated by islands and vegetation. Volume change has been analyzed for the main channel of each reach, as well as for all channels.

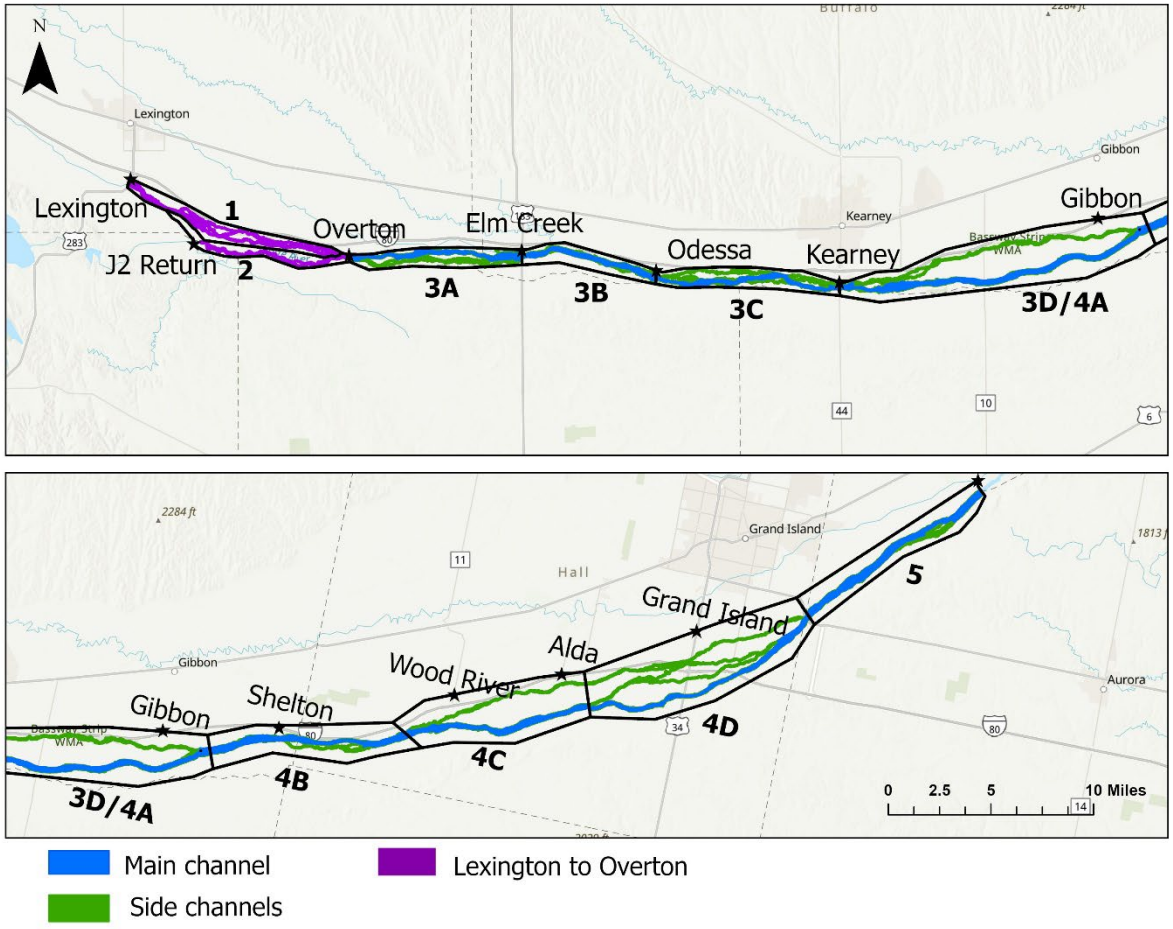

Figure 19. Geomorphic reaches used for the volume change analysis with the major bridges labeled with a black star.

Area-Averaged Change

As shown in **Figure 19**, the reaches considered in this analysis do not have consistent lengths or wetted areas. Larger volume change quantities are expected on larger reaches, simply due to their size. To control for this variation and make the reaches easier to compare to one another, we divided volume change by wetted area in each reach (see **Equation 1**). This calculation provides a standardized change value in units of vertical feet. Large positive or negative values of this metric indicate reaches that are changing more per square foot than others and thus may be experiencing higher levels of disequilibrium.

Equation 1: Area-Averaged Change = Volume Change (ft^3)/Wetted Reach Area (ft^2)

We also evaluated the time series of area-averaged bed elevation for each reach to identify any aggradation or degradation trends over time using the non-parametric Mann-Kendall test (Helsel and Hirsch, 1992). To guard against inflated Type I error caused by serial correlation, each series was first subjected to the trend-free pre-whitening procedure of Yue and Wang (2002). Detrended data showed no significant serial autocorrelation, leading us to analyze the original data series. The

mean magnitude and direction of change in each reach was estimated using Sen's slope estimator (Sen, 1968).

Results

Our volume change analysis offers another way to examine the dynamic nature of the river across the AHR. Some patterns of degradation have emerged over the past 8 years, while many changes (aggradational and degradational) are short lived.

Volume Change

Sediment volume loss from a river reach can indicate several geomorphic processes. Volume lost from the bed indicates channel deepening and potential disconnection from the surrounding floodplain. In the AHR, this is almost always undesirable. Volume lost from banks and islands due to horizontal stress (lateral erosion) can be a result of channel migration or width adjustment. Sediment that was previously stored in the bank is added to the system and incorporated into downstream bars, potentially reducing downstream deficits. Therefore, high lateral erosion is often a positive outcome on the AHR. This difference between bed and lateral erosion makes it important to evaluate change due to these processes separately. **Figure 20** provides a broad overview of the quantities of bed, lateral, and total erosion across the AHR for all channels since 2016.

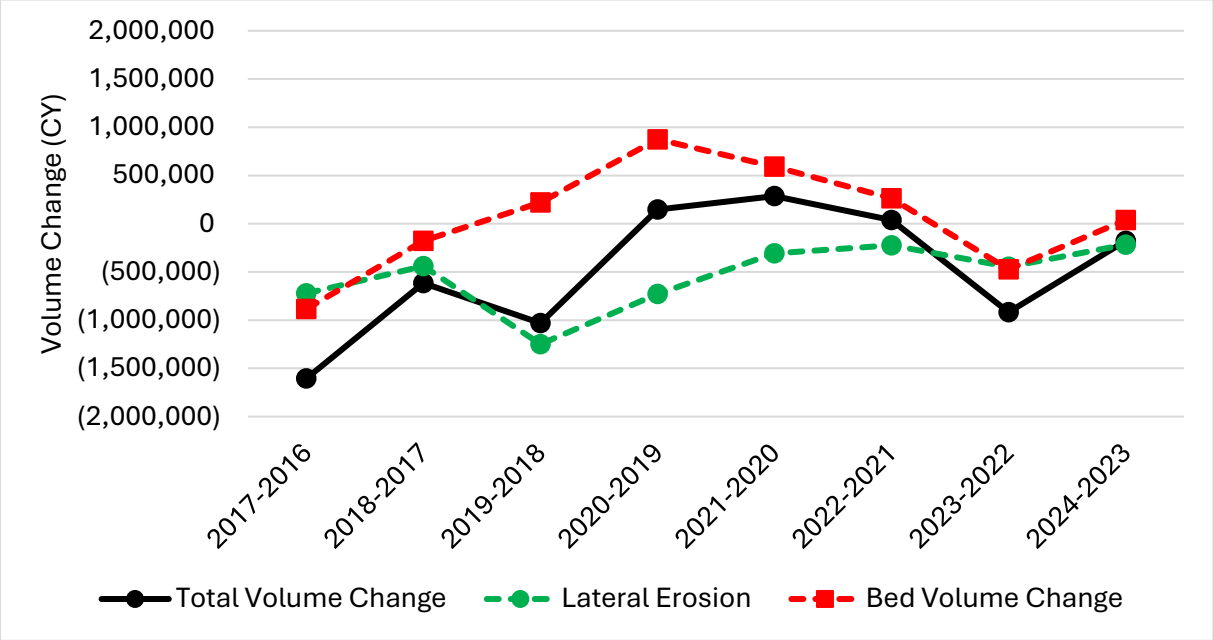

Figure 20. Annual sediment volume change for all channels in AHR (Lexington to Chapman) by year separated into total volume change, lateral erosion, and net bed volume change. Negative volume change (degradation) indicated in values below zero in parentheses.

A greater total volume of material has been lost than gained across all channels of the AHR in five out of eight monitoring years (black line). If volume loss due to lateral erosion is removed from this total, we observe five years where the AHR experienced more bed aggradation than erosion. This indicates that the riverbed in the AHR as a whole is maintaining a dynamic equilibrium, neither eroding nor aggrading consistently.

When volume change is examined at a reach-by-reach scale, as shown in the following tables, we observe more variability than indicated by the system-scale analysis. In some cases these changes swing from positive and negative year to year like reach 4B from Gibbon to Wood River. In other cases, a consistent pattern of total volume loss can be observed like in reach 2 (J2 Return Channel reach) and 3B from Elm Creek to Odessa (**Table 19**). No reach shows a consistent pattern of bed erosion (**Table 20**), meaning that lateral erosion (**Table 21**) is a meaningful component of volume change throughout the AHR. Removing lateral erosion shows that in four of the six years that sediment augmentation occurred, the J2 Return Channel reach experienced bed aggradation. Note Table 3 compares the magnitude of aggradation to the augmented volumes. The values do not match due to the combination of natural changes and sediment augmentation on the reach. For example, 2017-2019 experienced net bed degradation on the reach despite sediment augmentation.[9] This was likely due to high flows in those years. The most consistently degradational reaches were 3A and 3B spanning from the Overton Bridge to Odessa. The only year of net bed aggradation on reach 3B was 2019 to 2020. A levee breach near the Elm Creek Bridge on reach 3B increased bed and lateral erosion from 2022 to 2024.

Table 19. Total sediment volume change (CY) in the main channel by segment and year. Aggradation is in shades of green and degradation is in shades of red with negative values in parentheses.

Year	17-16	18-17	19-18	20-19	21-20	22-21	23-22	24-23	24-16
1	59,029	(26,485)	(6,771)	(21,523)	68,692	13,374	(152,397)	44,187	(24,746)
2	(138,150)+	(174,351)+	(221,029)+	(111,441)+	(95,721)+	(81,226)+	(85,480)	(101,206)	(980,552)
3A	(18,876)	(97,391)	(69,783)	(26,231)	19,058	(29,225)	(86,465)	(69,349)	(383,886)
3B	(81,321)	(109,231)	(111,236)	(29,235)	(27,344)	(28,853)*	(68,574)*	(41,958)*	(503,643)
3C	(33,115)	(105,226)	(108,030)	(13,544)	16,360	5,817	(64,580)	(5,845)	(323,854)
3D/4A	(115,901)	(165,813)	(81,620)	46,555	73,230	67,558	(159,073)	121,744	(230,510)
4B	(259,485)	110,359	(139,411)	105,415	25,093	38,678	(71,556)	(15,111)	(200,285)
4C	(252,508)	114,739	(133,737)	135,781	(8,298)	23,434	(65,993)	(66,103)	(266,698)
4D	(39,545)	(26,003)	(1,106)	81,427	17,204	24,534	(15,263)	(20,583)	16,378
5	(242,250)	(154,972)	(9,586)	(16,846)	58,545	(23,978)	(63,385)	(35,105)	(480,945)
Total	(1,122,122)	(634,372)	(882,310)	150,358	146,820	10,111	(832,765)	(189,328)	(3,378,740)

[9] For more information on sediment augmentation please see 2024 Sediment Augmentation Data Synthesis Compilation (PRRIP 2024).

Table 20. Bed volume change (CY) in the main channel by segment and year. Aggradation is in shades of green and degradation is in shades of red with negative values in parentheses.

Year	17-16	18-17	19-18	20-19	21-20	22-21	23-22	24-23	24-16
1	97,111	(7,417)	25,371	4,317	75,368	21,729	(54,075)	53,914	205,989
2	60,462+	(71,197)+	(104,620)+	1,216+	11,620+	3,409+	(20,246)	(51,557)	(108,267)
3A	6,397	(72,831)	(17,439)	6,631	35,651	(17,486)	(56,338)	(55,996)	(118,983)
3B	(48,526)	(88,353)	(45,233)	13,815	(7,001)	(12,367)*	(43,574)*	(30,767)*	(233,563)
3C	5,884	(73,519)	4,035	32,664	41,597	25,138	(23,546)	11,906	58,663
3D/4A	(55,505)	(130,992)	10,420	103,556	89,303	76,066	(143,819)	133,435	41,990
4B	(202,202)	146,910	(3,189)	163,256	44,739	50,711	(43,461)	115	189,791
4C	(215,656)	132,831	(80,320)	184,961	(2,880)	31,389	(52,326)	(50,913)	(58,794)
4D	(6,089)	(12,194)	42,401	128,615	27,768	31,374	(6,750)	(7,273)	156,828
5	(193,722)	(117,151)	132,643	69,126	78,871	(12,566)	(44,647)	(20,707)	(120,519)
Total	(551,845)	(293,912)	(35,929)	708,156	395,036	197,396	(488,780)	(17,844)	13,133

Table 21. Lateral erosion (CY) in the main channel by segment and year. Aggradation is in shades of green and degradation is in shades of red with negative values in parentheses.

Year	17-16	18-17	19-18	20-19	21-20	22-21	23-22	24-23	24-16
1	(38,082)	(19,068)	(32,142)	(25,840)	(6,676)	(8,355)	(98,322)	(9,727)	(230,735)
2	(198,612)+	(103,154)+	(116,409)+	(112,658)+	(107,341)+	(84,635)+	(65,234)	(49,648)	(872,285)
3A	(25,273)	(24,560)	(52,345)	(32,862)	(16,593)	(11,739)	(30,127)	(13,353)	(264,904)
3B	(32,795)	(20,878)	(66,003)	(43,050)	(20,343)	(16,486)*	(25,000)*	(11,191)*	(270,079)
3C	(38,999)	(31,707)	(112,066)	(46,208)	(25,237)	(19,321)	(41,034)	(17,751)	(382,516)
3D/4A	(60,397)	(34,820)	(92,040)	(57,000)	(16,073)	(8,508)	(15,254)	(11,691)	(272,500)
4B	(57,283)	(36,551)	(136,222)	(57,841)	(19,646)	(12,033)	(28,095)	(15,226)	(390,076)
4C	(36,852)	(18,093)	(53,417)	(49,181)	(5,417)	(7,956)	(13,668)	(15,190)	(207,904)
4D	(33,455)	(13,809)	(43,507)	(47,188)	(10,564)	(6,841)	(8,513)	(13,310)	(140,450)
5	(48,528)	(37,821)	(142,230)	(85,972)	(20,326)	(11,412)	(18,738)	(14,398)	(360,425)
Total	(570,277)	(340,460)	(846,381)	(557,799)	(248,216)	(187,285)	(343,985)	(171,484)	(3,391,873)

+ denotes a year/reach when sediment augmentation occurred.
* denotes year/reach when a levee breach occurred.

Area-averaged bed volume change

Averaging bed volume change by wetted area is helpful for monitoring change on reaches of varying length, highlighting changes that are large in proportion to the length of the reach. Lateral erosion is not included in these values and the units are feet, meaning that the value can be considered the average change to bed elevation in that reach over the given time period. **Figure 21** shows area-averaged bed change in the main channel over the full span of our monitoring data (2016 to 2024), and **Table 22** shows year-by-year change. In **Table 20**, the north channel from Lexington to Overton (reach 1) had a bed volume change gain of 205,989 cubic yards from 2016 to 2024. This is nearly twice the magnitude of the 108,267 cubic yard loss from J2 Channel (reach 2). However, when these results are normalized by area (**Figure 21**), we see nearly equal magnitudes of change per

area on reaches 1 and 2. This finding better emphasizes the dynamic nature of the J2 Channel which is losing a substantial amount of sediment for a short reach.

While **Table 22** shows that all reaches experienced years of net positive and negative volume change, **Figure 21** shows that reaches 2, 3A, and 3B (J2 Channel to Odessa) saw the greatest negative changes while several other reaches experienced overall positive change of similar magnitudes (reaches 1, 4B, and 4D). The consistently negative trend and higher magnitude changes observed at reach 3B and, to a lesser extent, 3A may indicate that these reaches are losing more sediment than they are gaining and changing more per square foot than other reaches. On reach 3B, this is partially explained by sediment loss due to the levee breach in 2022 that resulted in a large volume of sediment being diverted from the channel and deposited into an inactive sandpit.[10] These patterns match the raw volume change in **Table 19**, however, the comparative prominence of change on the large reaches like 4B and 5 is reduced.

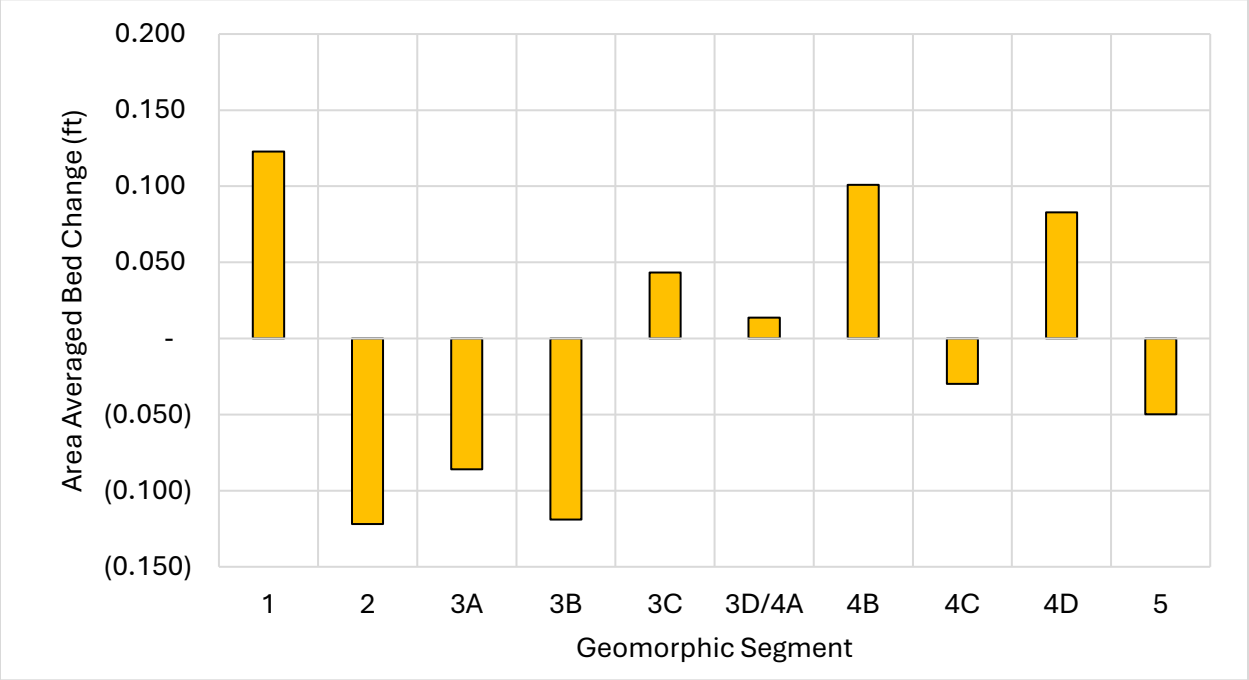

Figure 19. Total bed volume change normalized by the wetted area of the main channel in each reach from 2016 to 2024.

[10] The quantity of sediment diverted from the channel cannot be quantified because the depth of the mine is unknown. However, it is likely exceeds 500,000 cubic yards (filled estimated 15 acres with average depth of 20 ft).

Table 22. Total bed volume change normalized by the wetted area in the main channel by segment and year. Aggradation is in shades of green, degradation is in shades of red with negative values in parentheses.

Year/Reach	17-16	18-17	19-18	20-19	21-20	22-21	23-22	24-23	24-16
1	0.059	(0.005)	0.014	0.002	0.044	0.013	(0.031)	0.035	0.123
2	0.066	(0.070)	(0.119)	0.002	0.014	0.004	(0.023)	(0.056)	(0.122)
3A	0.005	(0.052)	(0.013)	0.005	0.025	(0.012)	(0.040)	(0.040)	(0.086)
3B	(0.033)	(0.060)	(0.031)	0.010	(0.005)	(0.009)	(0.012)	(0.018)	(0.119)
3C	0.004	(0.054)	0.003	0.024	0.069	0.018	(0.017)	0.008	0.043
3D/4A	(0.018)	(0.042)	0.003	0.035	0.030	0.026	(0.048)	0.044	0.014
4B	(0.107)	0.078	(0.002)	0.088	0.024	0.027	(0.029)	0.000	0.101
4C	(0.110)	0.067	(0.041)	0.095	(0.006)	0.016	(0.026)	(0.025)	(0.030)
4D	(0.003)	(0.007)	0.023	0.074	0.016	0.017	(0.004)	(0.004)	0.083
5	(0.079)	(0.048)	0.055	0.029	0.032	(0.005)	(0.018)	(0.008)	(0.050)
Total	(0.216)	(0.192)	(0.106)	0.363	0.242	0.094	(0.247)	(0.064)	(0.043)

The highest rate of degradation of -0.020 ft per year occurred in Reach 2 (J2 Return Channel) despite that segment experiencing slight bed aggradation in 50% of years. This due to the high magnitude of degradation that occurred in this segment in 2019. **Table 23** provides cumulative area-averaged bed volume change for the main channel over the period of 2016-2024. **Table 24** provides the results of the trend analysis for cumulative area-averaged bed volume change for the main channel over the same period. Five reaches show a statistically significant trend over that period. Reach 1, 3C, and 4D show a trend of increasing bed elevation (aggradation) and reaches 2, 3A and 3B show a significant decreasing (degradational) trend. The highest rate of aggradation (0.018 ft per year) occurred in Reach 4D, near Grand Island.

Table 23. Cumulative change in area-averaged bed volume through time in the main channel by segment and year. Aggradation in shades of green. Degradation in shades of red with values in parentheses. Bed volume of all reaches normalized to 0 in 2016 to show change through time from initial topo-bathymetric LiDAR survey.

Year	2016	2017	2018	2019	2020	2021	2022	2023	2024
1	0	0.059	0.054	0.068	0.071	0.114	0.127	0.096	0.131
2	0	0.066	(0.004)	(0.123)	(0.121)	(0.107)	(0.103)	(0.126)	(0.183)
3A	0	0.005	(0.047)	(0.060)	(0.055)	(0.030)	(0.042)	(0.082)	(0.122)
3B	0	(0.033)	(0.093)	(0.124)	(0.114)	(0.119)	(0.128)	(0.158)	(0.179)
3C	0	0.004	(0.049)	(0.046)	(0.022)	0.047	0.065	0.048	0.056
3D/4A	0	(0.018)	(0.060)	(0.057)	(0.022)	0.008	0.033	(0.014)	0.030
4B	0	(0.107)	(0.028)	(0.030)	0.058	0.081	0.108	0.079	0.079
4C	0	(0.110)	(0.042)	(0.083)	0.013	0.007	0.023	(0.003)	(0.029)
4D	0	(0.003)	(0.010)	0.013	0.087	0.102	0.120	0.116	0.112
5	0	(0.079)	(0.127)	(0.072)	(0.044)	(0.011)	(0.017)	(0.034)	(0.043)

Table 24. Analysis of statistical significance of trends in cumulative area-averaged bed change of main channel by reach for period of 2016-2024. Mann-Kendall used to identify statistically significant trends. Sen's slope used to estimate the slope (magnitude) of the relationship. Positive slope indicates aggradation. Negative slope indicates degradation.

	REACH									
Mann-Kendall	**1**	**2**	**3A**	**3B**	**3C**	**3D/4A**	**4B**	**4C**	**4D**	**5**
alpha	0.05	0.05	0.05	0.05	0.05	0.05	0.05	0.05	0.05	0.05
MK-stat	30	-22	-20	-32	20	14	19	8	24	6
s.e.	9.592	9.592	9.592	9.592	9.592	9.592	9.539	9.592	9.592	9.592
z-stat	2.606	-2.189	-1.981	--3.232	1.981	1.355	1.887	0.730	2.398	0.521
p-value	0.009	0.029	0.048	0.001	0.048	0.175	0.059	0.466	0.016	0.602
Trend	**YES**	**YES**	**YES**	**YES**	**YES**	**NO**	**NO**	**NO**	**YES**	**NO**
Sen's Slope										
alpha	0.05	0.05	0.05	0.05	0.05				0.05	
slope	**0.012**	**-0.020**	**-0.012**	**-0.010**	**0.010**				**0.019**	
lower	0.005	-0.034	-0.024	-0.027	-0.005				0.004	
upper	0.020	-0.002	-0.004	-0.008	0.023				0.026	

References

Baasch, D.M., Farrell, P.D., Howlin, S., Pearse, A.T., Farnsworth, J.M. & Smith, C.B., 2019. Whooping crane use of riverine stopover sites. PloS ONE 14(1).

Bankhead, N., 2012. Directed Vegetation Research: Lateral Bar Erosion Study. Platte River Recovery Implementation Program.

Blaschke, T., 2010. Object based image analysis for remote sensing. ISPRS Journal of Photogrammetry and Remote Sensing 65, 2-16.

Burnett, C. & Blaschke, T., 2003. A multi-scale segmentation/object relationship modelling methodology for landscape analysis. Ecological Modeling 168, 233-249.

Demarchi, L., Bizzi, S. & Piegay, H., 2016. Hierarchical Object-Based Mapping of Riverscape Units and in-Stream Mesohabitats using LIDAR and VHR Imagery. Remote Sensing 8, 97.

Department of the Interior (DOI), 2006. Biological Opinion on the Platte River Recovery Implementation Program.

Fansworth, J.M., Baasch, D.M., Farrell, P.D., Smith, C.B., & Werbylo, K.L., 2018. Investigating whooping crane habitat in relation to hydrology, channel morphology and a water-centric management strategy on the central Platte River, Nebraska. Heliyon, 4(10).

Fotherby, L.M., 2009. Valley confinement as a factor of braided river pattern for the Platte River. Geomorphology, 103(4).

Helsel, D.R. and R.M. Hirsch. 1992. Statistical methods in water resources. Studies in Environmental Science 49. New York: Elsevier. (available on-line as a pdf file at: http://water.usgs.gov/pubs/twri/twri4a3/)

Hydrologic Engineering Center (HEC), 2022. HEC-RAS, River Analysis System User's Manual, Version 6.3, CPD-68, U.S. Army Corps of Engineers, Davis, CA

Interagency Advisory Committee on Water Data, 1982. Guidelines for determining flood flow 52 frequency. Bulletin 17B of the Hydrology Subcommittee, Office of Water Data Coordination, U.S. Geological Survey (USGS).

Independent Science Advisory Committee (ISAC) 2014. Responses to Questions Posed by the Platte River Recovery Implementation Program (PRRIP) in October 2014.

McFeeters, S.K., 1996. The use of the Normalized Difference Water Index (NDWI) in the delineation of open water features. Remote Sensing Letters 17(7).

Murphy, P.J., Randle, T.J., Fotherby, L.M., Daraio, J.A., 2004. The Platte River Channel: History and Restoration. U.S. Department of the Interior, Bureau of Reclamation.

NV5, 2021. Platte River, Nebraska – Fall 2021: Topo-bathymetric LiDAR Technical Data Report

NV5, 2022. Platte River, Nebraska – Fall 2022: Topo-bathymetric LiDAR Technical Data Report

NV5, 2023. Platte River, Nebraska – Fall 2023: Topo-bathymetric LiDAR Technical Data Report

NV5, 2024. Platte River, Nebraska – Fall 2024: Topo-bathymetric LiDAR Technical Data Report

Platte River Recovery Implementation Program (PRRIP), 2017. Data Synthesis Compilation: Whooping Crane (*Grus americana*) Habitat Synthesis Chapters.

Platte River Recovery Implementation Program (PRRIP), 2022a. 2022 PRRIP Virtual Science Plan. Reporting Session – Independent Scientific Advisory Committee (ISAC) Discussion Questions.

Platte River Recovery Implementation Program (PRRIP), 2022b. *System-Scale Geomorphology and Vegetation Monitoring Report 2017-2020.* Platte River Recovery Implementation Program (PRRIP) Executive Director's Office (EDO).

Platte River Recovery Implementation Program (PRRIP) 2023. Data Synthesis Compilation: Sediment Augmentation.

Platte River Recovery Implementation Program (PRRIP), 2024. *Sediment Augmentation Data Synthesis Compilation.* Platte River Recovery Implementation Program (PRRIP) Executive Director's Office (EDO).

Platte River Recovery Implementation Program (PRRIP). 2025. Whooping Crane Riverine Roost Site Selection Update.

Quantum Spatial Inc. (QSI), 2016. Platte River, Nebraska – Fall 2016: Topo-bathymetric LiDAR Technical Data Report.

Quantum Spatial Inc. (QSI), 2017. Platte River, Nebraska – Fall 2017: Topo-bathymetric LiDAR Technical Data Report.

Quantum Spatial Inc. (QSI), 2018. Platte River Fall 2018, Nebraska: Topo-bathymetric LiDAR Technical Data Report.

Quantum Spatial Inc. (QSI), 2019. Platte River Fall 2019, Nebraska: Topo-bathymetric LiDAR Technical Data Report.

Quantum Spatial Inc. (QSI), 2020. Platte River Fall 2020, Nebraska: Topo-bathymetric LiDAR Technical Data Report.

Rouse, J.W., Haas, R.H., Schell, J.A. & Deering, D.W., 1973. Monitoring vegetation systems in the Great Plains with ERTS. NASA. Goddard Space Flight Center 3d ERTS-1 Symp., Vol. 1, Sect. A

Sen, P. K. (1968). Estimates of the Regression Coefficient Based on Kendall's Tau. *Journal of the American Statistical Association*, *63*(324), 1379–1389. https://doi.org/10.1080/01621459.1968.10480934

Tetra Tech, 2017. 2016 Platte River Final Data Analysis Report: Channel Geomorphology and In-channel Vegetation. Platte River Recovery Implementation Program.

Trimble, 2021. eCognition Version 10.2. https://geospatial.trimble.com/products-and-solutions/ecognition

United States Geological Survey (USGS) Monitoring Location. Platte River near Kearney, Nebraska – 06770500 Water Gage. https://waterdata.usgs.gov/monitoring-location/USGS-06770200/#dataTypeId=continuous-00065-0&period=P7D

United States Geological Survey (USGS) Monitoring Location. Platte River near Overton, Nebraska – 06768000 Water Gage. https://waterdata.usgs.gov/monitoring-location/USGS-06768000/#dataTypeId=continuous-00065-0&period=P7D

United States Geological Survey (USGS) Monitoring Location. Platte River near Grand Island, Nebraska – 06770500 Water Gage. https://waterdata.usgs.gov/monitoring-location/USGS-06770500/#dataTypeId=continuous-00065--2051167928&period=P7D

Yue, S. and Wang, C.Y., 2002. Applicability of prewhitening to eliminate the influence of serial correlation on the Mann-Kendall test. Water resources research, 38(6), pp.4-1.

Appendix to System-Scale Geomorphology and Vegetation Monitoring Report

Table of Contents

Appendix 1. Land Cover Classification and Unobstructed Width Protocol

Compile stock shapefiles used for analysis

1. Analysis Hull – in the past, we have used different analysis hulls to clip ecognition. We have decided to use a new analysis hull in 2024 and re-create ecognition land cover classification for 2017 – 2023. This hull was created by merging the 5,000 cfs masks from 2017 – 2022 and buffering this mask by 600 feet. I used the updated HEC-RAS masks located below
    a. S:\GIS\Masks\5000cfs_poly\HEC Updates
2. Ecognition Infrastructure – This mask is used to clip out all bridges and powerlines. This needs to be clipped out of the Analysis hull
    a. S:\GIS\Masks\Ecog_infrastructure.shp
3. Geomorphic Reaches – The analysis hull needs to be clipped by geomorphic reach to run ecog by reach and speed up the process
    a. Depending on how long you want ecognition to run, you can split it up by reach or combine reaches together. In 2024, the analysis hull was split into seven parts. Because the area is so much larger than previous years, many segments were needed to speed up the classification process
    b. S:\Users\Nicole Fijman\Ecog Masks Split
4. Cross-section lines – cross section of the river at 500 ft intervals that have been used since 2017, this file should include the Station ID
    a. S:\GIS\Masks\AHR_XS_Final.shp
5. 5,000 cfs polygon – This is created from the 2D modeling and should have one shapefile associated with each year.
    a. S:\GIS\Masks\5000cfs_poly\HEC Updates
6. Managed Area – polygon representing managed and unmanaged areas of the channel, this is used to report on unvegetated widths in each category
    a. S:\GIS\Base Data\PRRIP_Layers\ConsLands_2024.shp

Prepare Imagery and LiDAR rasters

1. Load fall topobathymetric and highest-hit LiDAR rasters
2. Using the Raster Calculator in the Spatial Analyst toolbar, subtract the Highest-hit from the Topobathymetric raster. This will produce a raster representing vegetation height
    a. I did this by clipping each of the four images separately – so highest hit_1 minus topobathymetric_1.
    b. When the raster is created, ensure the values make sense. There should be decimal places in the raster.
3. If you subtracted the rasters in four separate rasters, use Mosaic to New Raster to merge these four veg height rasters together.
    a. It is important that the raster is calculated to the decimal point, so make sure to use the 32 bit float for the pixel type
4. Clip the veg height raster to each section of the analysis hull and save as a .tif file

5. Load in mosaic tiles for fall imagery and merge tiles by geomorphic reach. Load in all tiles that cover the reach, save the file as a .tif. Degrade the image to 3ft by 3ft cell size and 4 total bands.
    a. If you use the same analysis hull, these are the tiles you need for each section
        i. AH1: 1710 – 1791
        ii. AH2: 1791 – 1866
        iii. AH3: 1866 – 1935
        iv. AH4: 1932 – 1989
        v. AH5: 1989 - 2055
        vi. AH6: 2049 – 2112
        vii. AH7: 2106 - 2169

<u>Run Classification in E-Cognition</u>

These steps relate to each step in ecognition.

1. Create / Modify Project:
    a. Create a new project and name it by year and reach, to start a new project, you have to load in imagery. You can load in the imagery for the year and geomorphic reach
    b. Set results folder to where you want results to be stored
    c. Add the geomorphic reach polygon and set it as the ROI
    d. Add the vegetation height raster and set it as the DSM
    e. Under spectral bands, set imagery band 3 to blue, imagery band 2 to green, imagery band 1 to red, and imagery band 4 to NIR.
    f. Select “Create Layers” to build NDWI, NDVI, and NDSI from the imagery in the project
2. Multiresolution Segmentation:
    a. Working domain – Pixel Level
    b. Algorithm – original multiresolution
    c. Scale – 10
3. Threshold Segmentation | Classification:
    a. Working domain – unclassified
    b. NDWI – 0.01
        i. Cut-off values may range from 0 – 0.1 between years. For each year of data, visually calibrate the cut-off values by iteratively testing values and comparing the classified area of water to the extent evident in RGB, CIR, and NDWI displays
    c. Class for dark – unclassified
    d. Class for bright – Water
        i. Will need to create a new class and choose a color for this class
4. Minimum Mapping Unit:
    a. Selected classes
    b. Classes – Water
    c. Minimum mapping unit pixels – 4
5. Threshold Segmentation | Classification:
    a. Working domain – unclassified

    b. Veg Height raster – threshold 15
    c. Class for dark – unclassified
    d. Class for bright – Veg > 15ft
        i. Will need to create a new class and choose a color for this class
6. Threshold Segmentation | Classification:
    a. Working domain – unclassified
    b. Veg Height raster – threshold 6
    c. Class for dark – unclassified
    d. Class for bright – Veg 6-15 ft
        i. Will need to create a new class and choose a color for this class
7. Threshold Segmentation | Classification:
    a. Working domain – unclassified
    b. Veg Height raster – threshold 2
    c. Class for dark – unclassified
    d. Class for bright – Veg 2-6 ft
        i. Will need to create a new class and choose a color for this class
8. Minimum Mapping Unit:
    a. Use "Selected Classes" and choose Veg 6-15 ft and Veg 2-6ft, don't add Veg 15+
    b. Minimum Mapping Unit pixels – 4
9. Threshold Segmentation | Classification:
    a. Working domain – unclassified
    b. NDVI – 0.3
        i. Cut off values from 2017 – 2020 ranged from 0.03 – 0.09 and values in the future may deviate from that range. For each year of data, calibrate the NDVI cut off value visually by iteratively testing values and comparing the classified area to displays
    c. Class for dark – Sand
    d. Class for bright – Veg < 2ft
        i. Will need to create a new class and choose a color for this class
10. Smooth Objects:
    a. All Classes
    b. Scale: 2
11. Export:
    a. Export type: Objects -> Vector
    b. Class filter: All Classes
    c. Attributes: Assigned class
    d. Export Name: Name your results – will be located in the results folder designated above
    e. Export format: .shp

<u>Compare Ecog to Validation data</u>

1. Merge analysis hull areas together to create one shapefile for the entire region
2. To assess how well ecog did, use the Spatial join tool to link the validation points to the merged ecog results polygon.

3. Export the shapefile into excel and create confusion matrices comparing field measured and ecog assigned classes for all points
    a. When creating the matrix, make sure all of your class names are the exact same and that the total number of points equal the number of points you have.
4. Check the agreement rate for all classes and for unobstructed vs obstructed values.
    a. If there seems to be a systemic bias towards one class or another, rerun Ecognition with adjusted values, this may be an iterative process with multiple repetitions

Calculate Unvegetated Widths

The procedure for calculating unvegetated widths has changed over time. To find a detailed review of what has happened 2017-2022 please refer to "Unvegetated Widths Historical Workflow".

We decided in 2024 to update and redo the unvegetated widths for years 2017 – 2022 using consistent procedures. The general steps are:

1. Results will be clipped to 5,000 cfs mask by year
2. Instead of comparing Main channel to all channel, we will be comparing all channels to all channels to keep measurements consistent.
    a. This will help us to determine where the largest unvegetated widths are, regardless of whether they are in the main channel shapefile or not
3. Cross sections will be clipped to unvegetated ecognition class types which includes sand, water, and vegetation less than 2 feet.
4. Vegetation widths will be compared for managed vs unmanaged sections of the river

Below are detailed directions for the analysis. These procedures can be found in the pycharm script that allows you to run these steps below for each year. The process takes around 5 minutes per year.

Detailed Directions:

- Save all of the baseline data in the same geodatabase and use consistent naming conventions
    - 5000cfs mask = c{year}_5000
    - eCognition file = eCognition_{year}
    - both cross section and main channel files can keep the original names - but must be saved in the gdb
    - AHR_XS
- Update working directory in the set geoprocessing environments
- Update the year of the assessment - only need to do this once
- Check that the ecognition file has the same "assigned_c" column name and the same unvegetated attributes listed below in step 3. If not, update these.

Data needed:

- 5000cfs mask for every year you are calculating unobstructed widths
- main channel shapefile
- cross section transects - one file to begin with
- eCognition results for every year you are calculating

Geoprocessing Steps:

1. Clip cross section shapefile to the 5,000cfs mask by year
2. Clip eCog results to 5000 cfs mask by year (both ecog and mask need to be the same year)
3. Create a new ecog file where the class type is considered unobstructed. These classifications are sand, water, and vegetation less than 2ft tall
4. Clip cross section by year file to unobstructed ecog file
5. Ensure there are no null values for any of the years - there should be the same about of transects for each year.
6. Repeat step 4, but clip eCog results to main channel shapefile after step. This will give us an analysis for both all channels and main channel unobstructed width

Calculate Management Status

After you create the unvegetated widths, you need to assign a management status to the unvegetated width segments.

1. Load in ConsLands_2024 and the main channel and all channel unvegetated width file that has the polylines exploaded.
2. Add a new column to the polyline file called "Management_status"
3. Using the polyline that is titled "split", use select by location tool to select all polylines that intersect with the consland shapefile.
    a. In the attribute table right click on the Management_status column and choose calculate field.
    b. Make sure that the only rows you are going to update are the ones that are selected. In the "Management_status =" box, put "Managed" and press ok. This will update all selected rows with a managed status.
4. Next we want to select the polylines that are within a specified distance of conservation land – for this example we will use 500 feet. Modify the select by location to be the exact same as before, but add in the "Search Distance" 500 and keep US Survey Feet.
    a. This will select fields that are both inside of the conservation land and within 500 feet. You don't want to overwrite the management status of "Managed". To avoid this, in the attribute table, click the "Switch" button for the selection. This will then switch the selection to everything else – not managed and not within 500 ft of conservation lands.
    b. Right click the column and use the Calculate field to add "Not managed" status to all of the selected fields.
5. Last we will add "Within 500 ft" management status. Click on select by attribute in the attribute table and write the statement shown below.
    a. This will select fields that do not currently have a status which will be fields that are within the buffer you set above.
    b. Right click the Management status column and use calculate field to add "Within 500 ft" to all of the selected fields.

You can now use management status to create figures for the Geomorphology Report.

Ecognition Mask Creation:

I created a new Ecognition mask to use for years 2017 to present. This was created by merging 5000 cfs masks from 2017 – 2022 and the analysis mask used for hydrologic modeling from Libby. This was to ensure that all areas that have been wet for the past 5 years were included in the map, as well as all areas that Libby uses as input to the model (meaning they are likely to be wet). This shapefile was buffered by 600 feet in hopes that the river will not change outside of this boundary for the next few years (excluding some sort of human influence that could change the river in an unnatural way). This was reviewed and approved by Nicole, Libby, Patrick, and Quinn.

Because this mask is larger, I did some testing with the 2018 ecognition creation. I ran ecog with the agg_deg_2018 mask and the updated mask and compared the validation point accuracy. I found that the accuracy increased with the larger mask. I do not think there will be an issue with decreasing accuracy because of this mask. To ensure this, I am also clipping out agricultural polygons from this file because they can be confused with sand and can interfere with classification. I have one file that was used historically that I will be updating in 2024 to ensure that changes in land use are captured in the shapefile.

Appendix 2. Comparison of SRH-2D to HEC-RAS 2D

Introduction

While a robust model, SRH-2D may no longer be the best choice for monitoring modeling. Since 2017, HEC-RAS 2D has continued to improve and gain users. HEC-RAS software now allows users to create meshes, run simulations, and visualize results in one open-source (free) package. SRH-2D requires different proprietary software to create meshes and visualize results, making it more expensive and complicated to use. There is also greater user support for HEC-RAS from its developers and large user base and HEC-RAS requires significantly less computational time than SRH-2D. Taken together, these factors make HEC-RAS a more attractive option, especially for new staff and program participants that need to work with models in the future.

Despite the apparent advantages of HEC-RAS 2D over SRH-2D, we must consider the potential impact of changing modeling platforms on our long-term monitoring trends. To determine what these impacts might be, we compared results from each model over three reaches and three flows. SRH-2D models have already been demonstrated to be adequately accurate, so our goal is to determine how HEC-RAS results will deviate from this standard. Several possible outcomes of this comparison exist, including:

A. HEC-RAS results are found to be less accurate than SRH-2D results. In this case no change should be made.
B. The difference between HEC-RAS and SRH-2D results is small enough to be considered insignificant, in which case a change to HEC-RAS can be made with no disruption to monitoring trends.
C. HEC-RAS results are found to have similar or greater accuracy than SRH-2D and are significantly different in such a way that monitoring trends will undergo a noticeable shift if a change is made. If a switch to HEC-RAS is made in this case, then comparisons with past data will require re-modeling past data using HEC-RAS.

Methods

The three reaches selected for this comparison were Grand Island to Chapman (GI_Chap), Odessa to Kearney (Od_Kea), and Lexington to Overton (Lex_Ov). The reaches come from different parts of the AHR (Fig. 2.1) and have distinctive geomorphic characteristics. GI_Chap is more consolidated and has fewer side channels than Od_Kea, while the J2 Return channel on the Lex_Ov reach is the only area of wandering rather than braided channel planform.

Figure 0.1 The AHR with selected reaches highlighted in red.

One HEC-RAS model was created for each reach. Domains were matched and the same 2022 LiDAR data was used to generate the bathymetry. The SRH-2D irregular meshes have an average cell spacing of 25-feet, so this was used as the average cell size used for the HEC-RAS models. Minimal breaklines were added at man-made boundaries such as bridges and levees to better align the cell edges with the flow direction. Manning's n values were matched as well as upstream and downstream boundary conditions. Matching these parameters as closely as possible allowed us to observe the effect of the computational differences between the models. Each model uses different forms and discretizations of the depth-integrated Navier-Stokes momentum and conservation equations. SRH-2D uses the Finite Volume Method (FVM) to solve for velocity and depth at each cell. In HEC-RAS 2D users can select from multiple solvers to fit different situations. The standard solver, referred to as the Shallow Water Equations (SWE) is similar to the method used in SRH-2D though a mixture of FVM and Finite Difference Methods (FDM) are used. Given the moderate slope of our reaches and our desire to model steady flows, the simplified Diffusion Wave Equation (DWE) solver was selected for this comparison. This solver ignores several terms in the momentum equation to reduce computation time and uses the FDM to solve for velocity and depth at each cell. The DWE often yields very similar results to the SWE solver, however, it is important to slowly ramp up to the desired steady flow using this method.

The three flows selected for this comparison were 500, 2,000, and 5,000 cfs. These constitute the lowest and highest flows considered in our monitoring analyses, as well as the flow at which critical hydrodynamic metrics like wetted width are calculated. The HEC-RAS models were run starting from a low flow of 10-20 cfs. Flows were then stepped up gradually using the previous step as the initial condition for the next. Each run lasted for 4-7 days of simulation time and required 1-2 hours to compute. For comparison, SRH-2D models are typically run for 2-3 days of simulation time and take more than 24 hours to compute. Once finished, simulation results were checked to ensure water levels and velocities had stabilized at the final flow level by generating time series graphs at various locations. Finally, raster depth and velocity results for each reach and flow were exported to GIS.

To compare the wetted area, depth, and velocities of HEC-RAS and SRH-2D, rasterized results were subtracted and differences summarized. Because HEC-RAS employs a "sub-grid" that interpolates results over the terrain beneath each grid cell, the resolution of results from the two models did not match. HEC-RAS results matched the resolution of the bathymetry data (3ft by 3ft),

while SRH-2D results had a resolution of 25ft by 25ft. This mismatch complicated our analysis, however, we concluded that performing an additional interpolation step would add further complications, so difference rasters were computed directly and assigned a resolution of 25ft by 25ft. Difference rasters of wetted extent, depth, and velocity were generated for each reach and flow.

Results

Wetted Extent

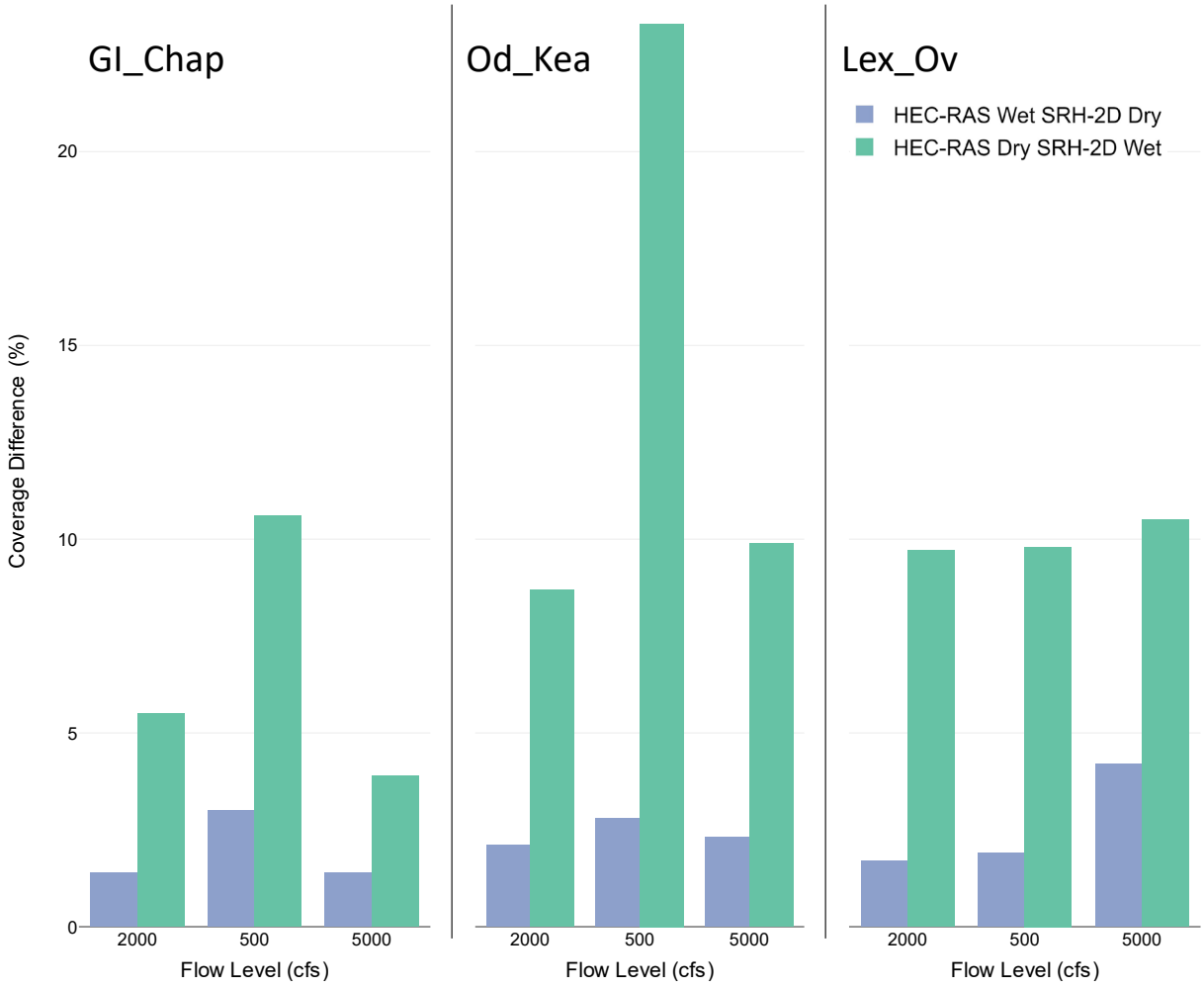

Figure 0.2 Percent of combined wetted area where there is disagreement between wet and dry areas. Blue bars represent areas wetted in HEC-RAS but dry in SRH-2D, while green bars represent areas dry in HEC-RAS but wet in SRH-2D.

Table 2.1 Disagreement between wet and dry areas, averaged over 500, 2000, and 5000 cfs flows.

Reach	Total Area (ac)	Average Area wetted in SRH-2D and not HEC-RAS (ac)	Average Area wetted in HEC-RAS and not SRH-2D (ac)
GI_Chap	1522	30	101

Od_Kea	1101	26	154
Lex_Ov	1330	34	130

The primary pattern observed in the wetted extent comparison is that the SRH-2D result rasters include a larger wetted area than the HEC-RAS result rasters. When viewed spatially, it becomes clear that this is partly due to the finer resolution of the HEC-RAS results. Because SRH-2D results are interpolated over 25 by 25-ft cells, any channels narrower than 25-ft are over-represented. In contrast, the HEC-RAS results can show much greater detail in wet and dry areas. Differences in resolution may also explain the larger area at the upstream end of the north Lexington channel that is wet in SRH-2D, dry in HEC-RAS (Figure 2.3). Both models develop inflow distributions along the upstream boundary cross-section based on normal depth, however, it seems that the reduced resolution in the SRH-2D model led to water being introduced at a higher elevation than HEC-RAS. The run that demonstrated the largest difference in wetted area was the Od_Kea reach at 500 cfs. Compared to the other runs that ranged from 0 – 10% difference, SRH-2D has over 20% more wetted area in this run, mainly over shallow bars in the main channel. Imagery captured during 500 cfs flows in 2022 indicate that these bars should be inundated. This indicates some inaccuracy in the HEC-RAS model at this flow that can likely be reduced with calibration.

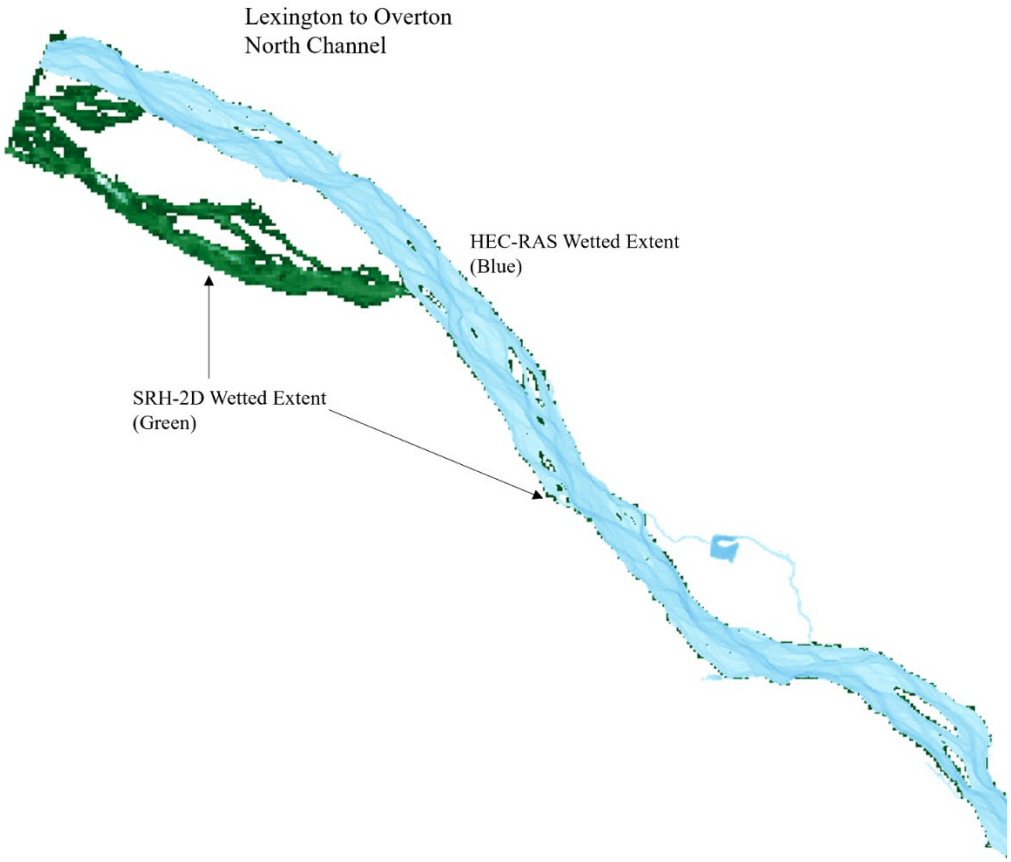

Figure 0.3 At the upstream end of the north channel near Lexington Bridge, the SRH-2D extent (green) is much broader than the HEC-RAS extent (blue). Roughly 3,000 ft downstream of the bridge, the two extents become very similar (green is under blue in this figure).

Depth

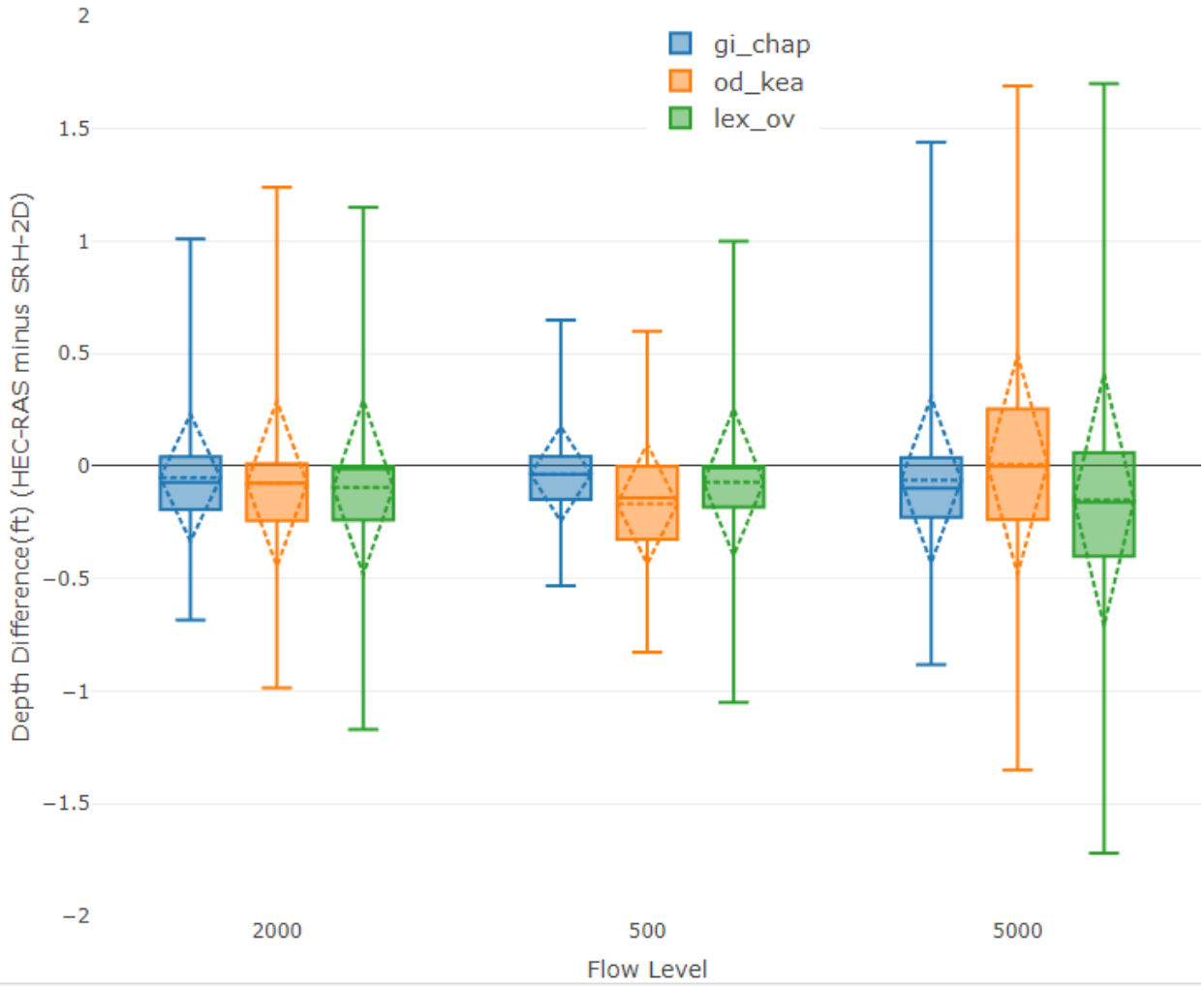

Figure 0.4 Results of subtracting SRH-2D depths from HEC-RAS depths. Negative results indicate that SRH-2D is deeper. Boxes represent the quartile range, dashed diamonds represent standard deviation, dashed and solid horizontal lines represent median and mean respectively. Upper and lower fences are the 99th and 1st percentiles.

Table 2.2 Depth differences averaged from 500, 2000, and 5000 cfs flow runs. Negative values indicate that SRH-2D is deeper.

Reach	Median	Mean	Std. Dev	Min	Max
GI_Chap	-0.07	-0.05	0.29	-2.31	3.39
Od_Kea	-0.07	-0.08	0.37	-3.71	6.14
Lex_Ov	-0.06	-0.11	0.42	-5.98	4.91

As shown in Table 2.4, some large differences (> 2ft) between SRH-2D and HEC-RAS occurred, primarily in areas where one model showed ponded water and the other one dry land. As depicted by the small quartile range, however, the vast majority of depth values were very similar between the two models, and 99-percent of differences fell below 2 feet (Figure 2.3). There is a slight tendency for SRH-2D to be deeper than HEC-RAS, possibly owing to the finer resolution and smaller wetted areas in HEC-RAS results.

Velocity

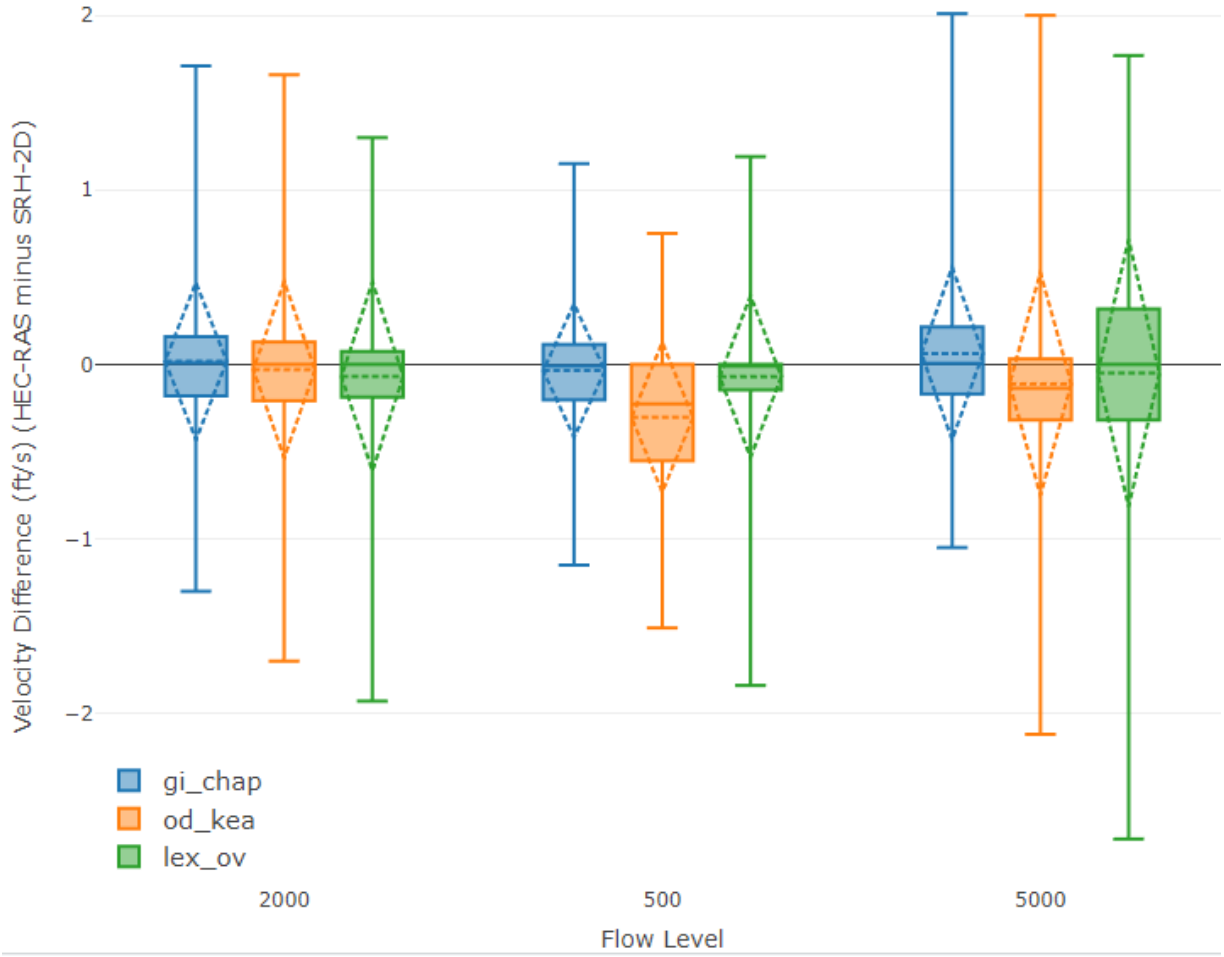

Figure 0.5 Results of subtracting SRH-2D velocities from HEC-RAS depths. Negative results indicate that SRH-2D is faster. Boxes represent the quartile range, dashed diamonds represent standard deviation, dashed and solid horizontal lines represent median and mean respectively.

Table 2.3 Velocity differences averaged from 500, 2000, and 5000 cfs flow runs. Negative values indicate that SRH-2D is deeper.

Reach	Median	Mean	Std. Dev	Min	Max
GI_Chap	0.00	0.02	0.44	-3.87	3.20

Od_Kea	-0.12	-0.15	0.52	-4.47	3.08
Lex_Ov	0.00	-0.06	0.59	-18.81	3.48

Figure 2.4 shows that, like with depth, differences in velocity between the SRH-2D and HEC-RAS models tend to be very small in the vast majority of locations. Table 2.5 shows that the Lex_Ov reach has a very large minimum difference of -18.81 ft/s, however this is a singular outlier at the upstream end of the J2 Return Channel. As flows increase, the possible range of velocities and velocity differences increases too, however, these differences often average close to zero. One exception to this is again the Od_Kea 500 cfs run in which the entire quartile range is below zero. This is likely something that could be addressed with calibration.

Hydrodynamic Metrics

As the final step of our comparison, we computed the monitoring metrics generated using hydraulic modeling data for the annual monitoring report. The values generated from HEC-RAS (HEC) and SRH-2D (SRH) results are presented in Table 2.6.

Table 2.4. HEC-RAS and SRH-2D hydrodynamic metrics calculated at 2,000 cfs.

	Wetted Width (ft)		Main Channel Avg. Depth (ft)		Main Channel W:D Ratio		% Main Channel Area < 1ft	
	HEC	SRH	HEC	SRH	HEC	SRH	HEC	SRH
GI_Chap	1053	1138	0.91	0.93	1157	1224	63	57
Od_Kea	760	849	1.20	1.21	634	702	25	22
Lex_Ov	524	620	1.34	1.32	391	470	46	46

As we can see from Table 2.6, there are differences between HEC-RAS and SRH-2D-generated monitoring metrics. HEC-RAS wetted widths tend to be smaller by 7 to 15% and W:D ratios smaller by 5 to 17%. Average depths are very similar (± 2%) and the percent of the main channel area below one-foot ranges from 0 -10% larger.

Discussion

Comparing the results of SRH-2D and HEC-RAS 2D over a range of flows and locations, the most significant differences stem from the difference in output resolution. The finer resolution of the HEC-RAS results lead to lower estimates of wetted area and subsequently wetted width and width-to-depth ratios. The majority of differences in depth and velocity were found to be very small (± 0.5 ft or ft/s), indicating that differences between the computational methods of the two models did not have a systematic impact on the results. If future modeling is conducted in HEC-RAS 2D, we expect to obtain higher precision by virtue of the finer resolution with a fraction of the time it currently takes to perform SRH-2D modeling. The consequence of switching from SRH-2D to HEC-RAS will likely be a noticeable departure from wetted width and width-to-depth ratio trends in future monitoring reports. In order to make these hydrodynamic metrics comparable starting in 2017, the 2017 – 2022 models would need to be re-run in HEC-RAS. This effort will begin after HEC-RAS models are created, calibrated, and validated for the entire AHR, likely by April 2024. After this

point modeling for the 2023 Monitoring Report will begin, starting with new data and working back to 2017.